

AD-A065 044

HARRIS CORP MELBOURNE FL ELECTRO-OPTICS DEPT  
AUTOMATIC CORRELATION MEASUREMENT EXPERIMENTS.(U)  
DEC 78 F B ROTZ, M W SHARECK

F/6 5/8

F30602-76-C-0381

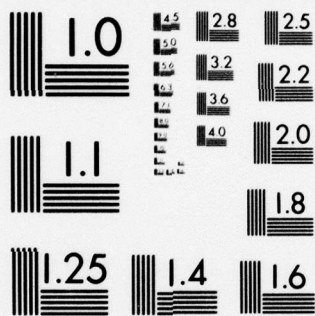
UNCLASSIFIED

RADC-TR-78-250

NL

1 OF 2  
AD  
A065044





MICROCOPY RESOLUTION TEST CHART  
NATIONAL BUREAU OF STANDARDS-1963-A



DDC FILE COPY

ADA065044

(12)

SC

LEVEL



RADC-TR-78-250  
Final Technical Report  
December 1978

## AUTOMATIC CORRELATION MEASUREMENT EXPERIMENTS

Harris Corporation

F. B. Rotz  
M. W. Shareck

APPROVED FOR PUBLIC RELEASE; DISTRIBUTION UNLIMITED

DDC  
REFILED  
FEB 28 1979  
RECEIVED

B

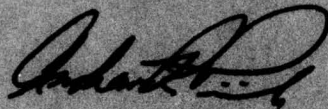
ROME AIR DEVELOPMENT CENTER  
Air Force Systems Command  
Griffins Air Force Base, New York 13441

79 02 23 050

This report has been reviewed by the RADC Information Office (OI) and is releasable to the National Technical Information Service (NTIS). At NTIS it will be releasable to the general public, including foreign nations.

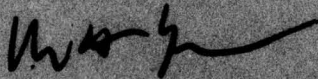
RADC-TR-78-250 has been reviewed and is approved for publication.

APPROVED:



ANDREW R. PIRICH  
Project Engineer

APPROVED:



ROSS H. ROGERS, Colonel, USAF  
Chief, Intelligence & Reconnaissance Division

FOR THE COMMANDER:



JOHN P. HUSS  
Acting Chief, Plans Office

If your address has changed or if you wish to be removed from the RADC mailing list, or if the addressee is no longer employed by your organization, please notify RADC (IRRR) Griffiss AFB NY 13441. This will assist us in maintaining a current mailing list.

Do not return this copy. Retain or destroy.



UNCLASSIFIED

SECURITY CLASSIFICATION OF THIS PAGE (When Data Entered)

REPORT DOCUMENTATION PAGE		READ INSTRUCTIONS BEFORE COMPLETING FORM
1. REPORT NUMBER RADCTR-78-250	2. GOVT ACCESSION NO.	3. RECIPIENT'S CATALOG NUMBER 9
4. TITLE (and Subtitle) AUTOMATIC CORRELATION MEASUREMENT EXPERIMENTS.	5. TYPE OF REPORT & PERIOD COVERED Final Technical Report.	
7. AUTHOR(s) F. B. Rotz M. W. Shareck	6. PERFORMING ORG. REPORT NUMBER N/A	
9. PERFORMING ORGANIZATION NAME AND ADDRESS Harris Corporation Electro-Optics Department Melbourne, FL 32925	8. CONTRACT OR GRANT NUMBER(s) F30602-76-C-0381	
11. CONTROLLING OFFICE NAME AND ADDRESS Rome Air Development Center (IRRE) Griffiss AFB NY 13441	10. PROGRAM ELEMENT, PROJECT, TASK AREA & WORK UNIT NUMBERS 62702F 55690148	
14. MONITORING AGENCY NAME & ADDRESS (if different from Controlling Office) Same	12. REPORT DATE December 1978	
16. DISTRIBUTION STATEMENT (of this Report) Approved for public release; distribution unlimited	13. NUMBER OF PAGES 117	
17. DISTRIBUTION STATEMENT (of the abstract entered in Block 20, if different from Report) Same	15. SECURITY CLASS. (of this report) UNCLASSIFIED	
18. SUPPLEMENTARY NOTES RADC Project Engineer: Andrew R. Pirich (IRRE)	15a. DECLASSIFICATION/DOWNGRADING SCHEDULE N/A	
19. KEY WORDS (Continue on reverse side if necessary and identify by block number) Image Matched Filter Optics Lasers Parallax	<div style="border: 2px solid black; padding: 5px; text-align: center;"> <b>DDC</b>  <b>RECEIVED</b>  <b>FEB 28 1979</b>  <b>RECEIVED</b>  <b>B</b> </div> <p>parallax</p>	
20. ABSTRACT (Continue on reverse side if necessary and identify by block number) This exploratory development describes a continuing effort to develop coherent optical processing techniques applicable to the automatic <del>appraisal</del> measurement process. An attempt to develop a feature extraction process employing the Image Matched Filter (IMF) system produced insignificant results and may warrant further investigation.		

DD FORM 1 JAN 73 1473

EDITION OF 1 NOV 65 IS OBSOLETE

UNCLASSIFIED

SECURITY CLASSIFICATION OF THIS PAGE (When Data Entered)

392 092

LB

## TABLE OF CONTENTS

Section		
	ABSTRACT . . . . .	iii
	PREFACE . . . . .	iv
I	INTRODUCTION . . . . .	1
II	RESULTS AND CONCLUSIONS . . . . .	4
	2.1 Summary of Results . . . . .	4
	2.2 Conclusions and Recommendations . . . . .	7
III	PRINCIPLES OF OPTICAL DATA PROCESSING . . . . .	9
	3.1 Coherent Optical Processing Techniques . . . . .	9
	3.2 Cross-Correlation Processing for Parallax Measurement . . . . .	19
	3.3 Optical Data Processing for Feature Extraction . . . . .	20
IV	CORRELATION DETECTION DEVICES . . . . .	23
	4.1 Output Sensor Requirements . . . . .	23
	4.2 Operational Principles . . . . .	26
	4.3 Device Trade-Off Analysis and Selection . . . . .	29
V	IMF SYSTEM CONFIGURATION . . . . .	35
	5.1 IMF System Description . . . . .	35
	5.1.1 IMF Optical Subsystem . . . . .	39
	5.1.2 IMF Electronic Subsystem . . . . .	44
	5.1.3 IMF Software Control Functions . . . . .	50
	5.2 IMF System: Development Results and Status . . . . .	57
VI	FEATURE EXTRACTION . . . . .	73
	APPENDIX A . . . . .	87
	APPENDIX B . . . . .	97/98

## LIST OF ILLUSTRATIONS

<u>Figure</u>		
3-1	Variable Scale System . . . . .	11
5-1	Functional Schematic of the IMF System . . . . .	37
5.1.1-1	IMF Optical Subsystem . . . . .	40
5.1.1-2	IMF Optical Subsystem - Data Collection Mode . . .	41
5.1.2-1	Functional Schematic of the IMF Electronic Subsystem . . . . .	47
5.2-1	IMF and AS11 Parallax data for Canadian Test Model . . . . .	60
5.2-2	Tracking Accuracy and Video Signal for Input Correlation Peak of 25 mV . . . . .	64
5.2-3	Tracking Accuracy and Video Signal for Input Correlation Peak of 100 mV . . . . .	65
5.2-4	Tracking Accuracy and Video Signal for Input Correlation Peak of 200 mV . . . . .	66
6-1	Image and Power Spectrum of Typical Urban Area . . . . .	80
6-2	Image and Power Spectra of Airway Landing Facility . . . . .	81
6-3	Image and Power Spectra of Rural Terrain . . . . .	82



# ABSTRACT

This final report describes a continuing effort to develop coherent optical processing techniques applicable to parallax measurement. The IMF system, an experimental coherent optical processor, was modified to automate the parallax measurement process. A CID camera system was procured and installed in the experimental system. Used with phase, rather than amplitude, matched filters, the CID camera provides adequate sensitivity for correlation detection with lower video noise levels and a fixed metric field. An electronic interface, capable of automatic correlation peak detection, was designed, fabricated, and tested. This interface and the associated control software was consistent with parallax data collection rates of 30 samples per second. A preliminary evaluation of the IMF system for pattern recognition was performed. Differences in the power spectral density were observed for urban and rural regions. The discrimination provided by a simple feature (power spectral density) merits continued investigation (a concentrated study to evaluate the effectiveness of coherent optical techniques for feature extraction and pattern recognition is warranted).

ACCESSION for		
NTIS	Write Section	<input checked="" type="checkbox"/>
DDC	Buff Section	<input type="checkbox"/>
UNANNOUNCED		<input type="checkbox"/>
JUSTIFICATION		
BY		
DISTRIBUTION/AVAILABILITY CODES		
Dist.	Avail. and/or	SPECIAL
A		

## PREFACE

This report was prepared by the Electro-Optics Department of the Harris Government Communication Systems Division, Melbourne, Florida, under Contract F30602-76-C-0381 with Rome Air Development Center, IRRE, Griffiss Air Force Base, Rome, New York; the effort was monitored by A. Pirich of RADC.

The Principal Investigator and Program Manager was F. B. Rotz, who reports to A. Vander Lugt, Director of the Electro-Optics Department. The major contributors to this report are M. W. Shareck and F. B. Rotz; K. R. Porter assisted in the experimental effort.

## EVALUATION

This report summarizes the findings of a continuing program to determine and provide improvements to an Image-Matched Filter (IMF) Correlator System.

The current phase of development has been primarily concerned with three areas:

a. The identification of a solid-state imaging device for correlation detection.

b. Implementation of an electronic interface for automatic correlation location.

c. Development of software for parallax collection at 30 samples per second.

Standard vidicons, charge-coupled devices, and charge-injection devices were evaluated for possible use as an output correlation detector. The charge-injection device (CID) was used and provided adequate sensitivity for correlation detection with low video noise levels and a fixed metric field.

Control Software for the PDP-8A computer was developed for IMF system operation at a rate of 30 samples per second. Computer routines to provide galvanometer control, aperture



location and movement, and correlation peak detection were written for the programmable control unit. The investigation into the possibility of employing the IMF system for pattern recognition and feature extraction was rather weak. The report definitely does not indicate a full appreciation of feature extraction/pattern recognition technology. Sorting the differences of the Power Spectrum from a few aerial scenes does not constitute a feature extraction/pattern recognition investigation. A portion of this effort was to explore the facets of optical versus digital image processing by employing the IMF Correlation System. This was not fully accomplished nor discussed within this report.

Comparison of the feature extraction and pattern recognition capabilities between digital and coherent optical systems is warranted.



ANDREW R. PIRICH  
Project Engineer

## SECTION I

### INTRODUCTION

The extraction of elevation data from stereoscopic aerial photographs requires determining with high accuracy the parallax associated with distinct terrain regions. This parallax, generated by a change in viewing angle, is the relative displacement of an object in the two stereo scenes. Originally, the parallax was measured by manual stereo-plotters and stereo-comparitors and subsequently reduced to obtain elevation and contour information. Over the past two decades, several automatic stereo-compilation systems have been developed utilizing modern electronic techniques. In general, these systems rely on a one-dimensional correlation scheme. In this scheme, the aerial photographs comprising the stereo pair are scanned with a small beam; the video signals resulting from the scanning process are electronically cross-correlated to determine the parallax.

Although these electronic correlation systems have been increasingly successful, improvements in operational performance, speeds, and costs are possible. The Rome Air Development Center (RADC) has been instrumental in exploring alternative approaches for stereocompilation which avoid the limitations of the electronic schemes. In particular, coherent optical data processing techniques offer advantages for both parallax

measurement and feature extraction. This final report describes a continuing effort to develop coherent optical processing techniques applicable to parallax measurement.

A key advantage of a coherent optical system is the direct presence of both an input scene and its Fourier transform within the same processor. Thus, either the image or its transform can be accessed. In addition, the system can perform a two dimensional cross-correlation between an input scene and a stored reference pattern.

Under a previous contractual phase, RADC assembled an Image Matched Filter (IMF) system, a large aperture coherent optical processor containing the components necessary for parallax measurement. On this system, the basic suitability of optical processing techniques for parallax measurement was demonstrated in a manual mode by the Electro-Optics Department of Harris Government Communication Systems Division. Subsequent effort was directed to refine and improve the breadboard system. During this phase, the complexity of the optical system was significantly reduced without sacrificing performance, scanning accuracy was improved, and automatic techniques for scanner calibration were demonstrated. In addition, preprocessing techniques developed for the input images increased the uniformity of the correlation process.



The work described in this report is a continued effort to automate and develop various techniques for processing aerial imagery with the IMF system. The specific objectives for this contract (F30602-76-0381) were:

- Evaluate sensors, including CCD, CID, and TV raster scanners, to determine the optimum correlation detection device.
- Develop an experimental system capable of collecting parallax data from vertical frame photography at rates of 30 samples per second, and
- Provide a methodology to extract cultural and terrain features from aerial photographs with the IMF system.

This report details the activities performed to complete these objectives. Our results and conclusions, along with recommendations for future activities, are summarized in Section II. A basic review of the theory of optical data processing is presented in Section III; a discussion of the potential advantages offered by a coherent optical system for stereocompilation and feature extraction is also included. The capabilities and performance offered by various area detection devices are summarized in Section IV; the optical and electronic system operations are described, as well as the software control functions. A description of a technique applicable to feature extraction is presented in Section VI.

## SECTION II

### RESULTS AND CONCLUSIONS

In this section, we briefly review the results and conclusions of our investigation and present our recommendations for future activity. Relevant supporting material is contained in subsequent sections of this report. A complete discussion of solid state image detectors is given in Section IV, while Section V describes the present developmental status of the IMF system. The potential of a coherent optical processing system for feature extraction is detailed in Section VI.

#### 2.1 SUMMARY OF RESULTS

Previous experimental evaluation of the IMF system has demonstrated the effectiveness of coherent optical processing for stereocompilation; parallax data obtained on the IMF system showed good agreement with corresponding data from the AS-11B system (Final Technical Report for Contract F30602 - 73 - C - 0312). Additional contract effort was initiated to improve several areas of concern. In this continued activity, the complexity of the optical system was reduced significantly, the stability and accuracy of the scanning system was improved, the correlation performance of input imagery was increased, and real-time spatial filter recording materials were investigated. A complete discussion of these results are contained in

the Final Technical Report for Contract F30602 - 75 - 0305.

The current phase of system development has been primarily concerned with three areas: the identification of a solid state imaging device for correlation detection, the implementation of an electronic interface for automatic correlation location, and the development of software for parallax collection at 30 samples per second. In addition, the potential of the IMF system for feature extraction was investigated.

Current area imaging detectors, including standard vidicons, charge-coupled devices, and charge-injection devices, were evaluated for possible use as an output correlation detector. Based on present performance levels and a random access capability, the charge-injection device (CID) was selected. A CID camera system was procured and installed in the breadboard system. Used with phase, rather than amplitude, matched filters, the CID camera provides adequate sensitivity for correlation detection with lower video noise levels and a fixed metric field.

An electronic interface providing the processing functions for automatic correlation peak detection was designed, fabricated and tested. Although the electronic interface performed well in the static test mode, several effects limited the performance in a dynamic mode. The cause for the limited performance was established, and two possible corrective actions were



identified. The interface, while not providing the potential accuracy of which it is capable, did prove the feasibility of collecting parallax data at 30 samples per second.

Control software required for system operation at these rates was developed. Computer routines to provide galvanometer control, aperture location and movement, and correlation peak detection were written for the programmable control unit. With the solid state detector array in the system, execution times were consistent with data collection rates of 30 samples per second. In addition, data handling and storage were provided at these execution rates.

A preliminary evaluation of the IMF system provides a direct access to the input imagery, its Fourier transform, and a spatially filtered version of the imagery. Although the potential value of these functions can be established only through an in-depth statistical study, initial estimates of their effectiveness were obtained. One example was power spectral analysis; the energy distribution of power spectral density is dependent on scene content and structure. Significant differences in the power spectral density were observed for urban and rural regions, indicating a relatively simple feature (such as the power spectrum) can be effective for terrain classification. Additional discussion is provided in Section VI.

## 2.2 CONCLUSIONS AND RECOMMENDATIONS

The indications of the experimental effort to date and the potential of the IMF concept in terms of cost and flexibility justify further system investigation. This is particularly true with the increasing demand for an automated pattern recognition scheme.

Several areas for improvement have been established during the present effort. To provide reliable operation, the scanning system should be refurbished. Although the existing scanning system provided good performance in the past, these units are due for replacement. The existing open-loop galvanometers should be upgraded with closed-loop, temperature regulated units. This will provide a significant increase in scanning accuracy, as well as improving system reliability. This upgrade is warranted for both stereocompilation and feature extraction.

The electronic interface designed and fabricated for correlation detection should be modified to correct and improve performance in the dynamic mode. Additional flexibility should be provided to use this modified interface for both stereocompilation and pattern recognition experiments.

In addition, the possibility of using an optical processor for pattern recognition from aerial photographs should be thoroughly investigated.



The IMF system contains the basic elements required for such an investigation. A concentrated, continuous study is necessary to evaluate the effectiveness of coherent optical processing for both feature extraction and pattern recognition.

### SECTION III

#### PRINCIPLES OF OPTICAL DATA PROCESSING

Coherent optics have a natural application to the processing of two-dimensional imagery. In contrast to digital computing, coherent optics directly provides parallel processing of large quantities of data and is ideally matched to sequential frame aerial photography. Aerial photographs contain a tremendous amount of information, typically over  $10^8$  bits per frame. This amount of information is easily handled by an optical system, but represents a significant problem for digital techniques in terms of both storage requirements and processing speeds. In addition, since the optical system is an analog processor, quantizing and digitizing errors are not encountered. In this section we discuss the basic principles of a coherent optical processing system.

##### 3.1 COHERENT OPTICAL PROCESSING TECHNIQUES

Incoherent and coherent illuminated optical systems have both been used for optical processing. The advent and development of the gas laser made coherently illuminated systems practical and superior in performance to incoherently illuminated systems. The ability of a coherent optical system to project a direct image, to display a Fourier transform, and to perform a correlation simultaneously are key advantages.

It is often desirable to change the scale of the transform in a coherent optical system. This provides a means of varying the relative scale of two functions for optical filtering. Various methods to scale the transform exist, such as a variable focal length lens. A particularly simple method is to employ a convergent beam geometry to perform the transform operation. This geometry is utilized in the IMF system and can readily provide a scale change of  $\pm 10\%$ .

The basic elements of a coherent optical processing system, as implemented in the IMF system, are shown in Figure 3-1. In describing the operation of the system, we assume that photographic transparencies are used to input the data for processing and to record the filters for correlation or spectrum weighting. A point source of monochromatic light is collimated by lens  $L_c$  and subsequently converged to plane  $P_2$  by the transform lens  $L_o$ , passing through a transparency with transmittance  $t(x)$ . The lens  $L_2$  images plane  $P_1$  into plane  $P_3$ ; in the system, the relative positions of  $P_1$ ,  $L_2$ , and  $P_3$  are kept constant as the distance  $l$  is varied.

For the one-dimensional case, the light amplitude after passage through the transparency is the product of a converging wave and the transmittance  $t(x)$ . This amplitude, denoted as  $A(x)$ , can be represented by



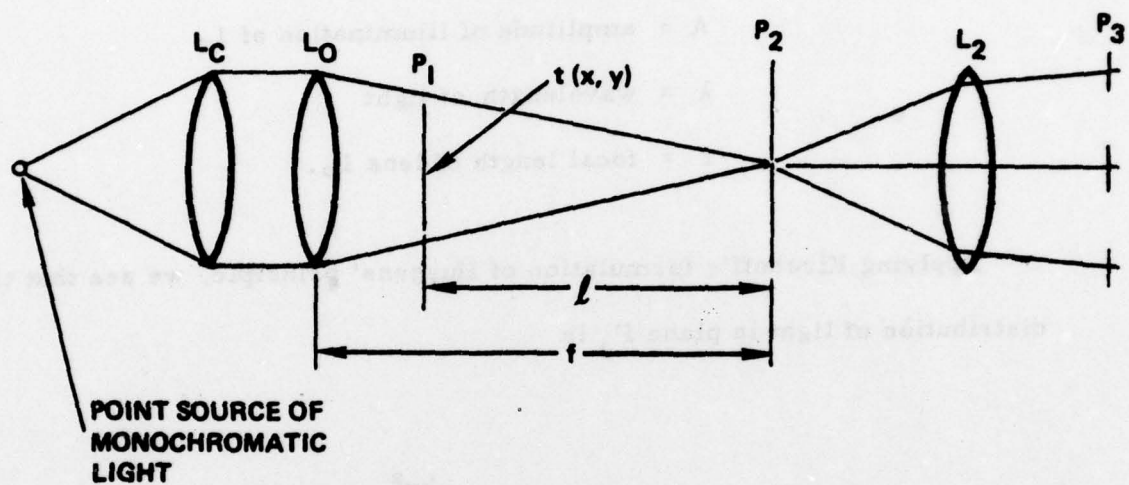


**Figure 3-1 Variable Scale System**

$$A(x) = \frac{Af}{\ell} t(x) \exp \frac{-j k x^2}{2\ell},$$

where

$$k = \frac{2\pi}{\lambda}$$

$A$  = amplitude of illumination of  $L_0$

$\lambda$  = wavelength of light

$f$  = focal length of lens  $L_0$ .

Applying Kirchoff's formulation of Huygens' principle, we see that the distribution of light in plane  $P_2$  is

$$T(\xi) = \sqrt{\frac{-j}{\lambda \ell}} \frac{f}{\ell} A \int_{P_1} \frac{t(x)}{r} e^{j \frac{k x^2}{2\ell}} e^{j k r \left( \frac{1 + \cos \theta}{2} \right)} dx,$$

where  $r$  is the distance from a point  $x$  in plane  $P_1$  to a point  $\xi$  in plane  $P_2$  and the term  $(1 + \cos \theta)/2$  is the obliquity factor.

Because the field angle  $\theta$  is small, we make the assumption that the obliquity factor  $(1 + \cos \theta)/2$  is approximately one. Using the binomial expansion, the distance  $r = (\ell^2 + (\xi - x)^2)^{1/2}$  can be represented

$$r = \ell \left[ 1 + \frac{1}{2} \frac{(\xi - x)^2}{\ell^2} - \frac{1}{8} \frac{(\xi - x)^4}{\ell^4} \dots \right].$$

Assuming  $\ell$  is much greater than  $\xi$  or  $x$  allows us to retain only the first two terms of the expansion; in addition, since the first term represents a constant reference phase, it is dropped from the analysis.

The expression for  $T(\xi)$ , the amplitude distribution in plane  $P_2$ , then becomes

$$T(\xi) = \sqrt{\frac{-j}{\lambda \ell}} \frac{fA}{\ell} \int_{P_1} \frac{t(x)}{\ell} e^{j \frac{kx^2}{2\ell}} e^{-j \frac{k(\xi - x)^2}{2\ell}} dx,$$

where we have observed that  $1/r$  varies slowly in comparison to the integrand. The phase terms in  $x^2$  cancel, allowing the simplification

$$T(\xi) = \frac{Af}{\ell^2} \sqrt{\frac{-j}{\lambda \ell}} e^{j \frac{k\xi^2}{2\ell}} \int_{P_1} t(x) e^{-j \frac{k\xi x}{\ell}} dx.$$

The integral must be performed over the effective aperture in plane  $P_1$ ; this is thus a function of  $\ell$ , the separation between the transparency and the transform plane. We require that the half-aperture  $W$  of lens  $L_0$  be large enough to illuminate the signal  $t(x)$  for all  $\ell$  of interest. The effective

aperture size in the transparency plane  $P_1$  is then simply  $W\ell/f$ . Inserting these limits of integration into the expression for  $T(\xi)$  yields

$$T(\xi) = g(\xi, \ell) \int_{-W\ell/f}^{W\ell/f} t(x) e^{j \frac{k\xi x}{\ell}} dx,$$

where

$$g(\xi, \ell) = \sqrt{\frac{-j}{\lambda\ell}} \frac{A}{\ell^2} e^{j \frac{k\xi^2 \ell}{2\lambda}}.$$

The expression for  $F(\xi)$  can be arranged into a transform type relation with the variable change  $x = \mu\ell/f$ ; this results in

$$T(\xi) = \frac{\ell}{f} g(\xi, \ell) \int_{-W}^W t(\mu\ell/f) e^{j \frac{k\xi\mu}{f}} d\mu.$$

Since  $t(\mu\ell/f)$  vanishes for  $|x| > W$ , the limits on the integral can be extended to infinity.  $T(\xi)$  and  $t(\mu\ell/f)$  then form a Fourier transform pair. The phase factor  $g(\xi, \ell)$  is expected since the signal is not in the front focal plane of  $L_0$ . With this system there is no limit on either the frequency response or the region of space-invariant operation, whereas when the signal is placed in front of  $L_0$ , there is a definite limit on both these quantities.

Spherical aberration due to the glass plates used to enclose the signal can be



compensated by proper design of lens  $L_0$ , since it is not a function of  $\ell$ . However, we note that, for the IMF system, the spherical aberration is not a significant factor. In fact, the convergent beam geometry generates less aberration than the previous conventional set up employing the custom transform lens.

From the transform relationship it is clear that the effective scale of the input signal varies inversely as  $\ell$  and the size of the transform varies directly as  $\ell$ . This is precisely the relationship desired, since we wish to vary the size of the transform with respect to a fixed scale in plane  $P_2$ . A spatial filter having an amplitude transmittance  $S(\xi)$  can be placed in plane  $P_2$  to modify the transform  $T(\xi)$  directly; this capability is used for performing a correlation operation. Alternately the Fourier transform is available for direct examination or spectrum weighting. The spectrum weighting functions available include differentiation, bandpass filtering, and edge-enhancement.

The amplitude  $r(u)$  of the light in the output plane  $P_3$  of the optical system is the Fourier transform of the wavefront emerging from the filter,

i. e.

$$r(u) = \frac{1}{2\pi} \int_{P_2} S(p) T(p) e^{-jpu} dp$$



where the spatial frequency variable  $p$  is related to the space coordinate  $\xi$  in plane  $P_2$  by

$$p = \frac{2\pi\xi}{\lambda f} .$$

Here for simplicity, the focal lengths of lens  $L_2$  and  $L_0$  are assumed to be identical and are denoted by  $f$ .

This relationship for  $r(u)$  can be used to perform a correlation operation between two functions  $t_1(x)$  and  $t_2(x)$  the filter function required can be generated as a spatial frequency carrier filter; the filter can be formed with the same optical system shown in Figure 3-1. The reference transparency  $t_1(x)$  is placed in plane  $P_1$  and illuminated by the convergent wavefront produced by lens  $L_0$ . The Fourier transform  $T_1(p)$  of the transparency is displayed in plane  $P_2$ . An off-axis reference beam of collimated light is incident on plane  $P_2$  at an angle  $\alpha$ ; this beam is represented by  $R \exp(jpb)$ , where  $b = f_2 \sin \alpha$ . The irradiance produced in plane  $P_2$  is denoted by  $S(p)$  and can be represented

$$\begin{aligned}
|S(p)|^2 &= |R \exp(jpb) + T_1(p)|^2 \\
&= R^2 + |T(p)|^2 + R \exp(-jpb) T_1(p) + R \exp(jpb) T_1^*(p)
\end{aligned}$$

This resultant interference pattern  $|S(p)|^2$  is recorded on a suitable recording medium, such as a high resolution photographic film or a photo-plastic material. Materials of these types typically exhibit an amplitude transmittance  $T_a$  which is linear in exposure  $E$ ; the  $T_a$ - $E$  curve for the material is characterized as

$$T_a = T_0 - \beta E,$$

where  $T_0$  is the amplitude intercept,  $\beta$  is the slope of the linear portion of the  $T_a$ - $E$  curve, and  $E$  represents the exposing irradiance. Thus, after the recording material is exposed and processed, its amplitude transmittance  $T_a(p)$  is

$$\begin{aligned}
T_a(p) &= T_0 - \beta |S(p)|^2 \\
&= \beta \left[ T_0/\beta - R^2 - |S(p)|^2 - \beta R T_1(p) \exp(jpb) \right. \\
&\quad \left. - \beta R T_1^*(p) \exp(-jpb) \right]
\end{aligned}$$

After processing, the filter is replaced in the optical system and is illuminated by  $T_2(p)$ , the Fourier transform of a second transparency  $t_2(x)$ . In the output plane  $P_3$  of the processor, we observe three filtered versions of the input data:

$$r_1(-u) = \frac{\beta}{2\pi} \int T_1(p) [T_0/\beta - R^2 - |T_1(p)|^2] e^{-jpu} dp,$$

$$r_2(-u) = \frac{R\beta}{2\pi} \int T_1(p) T_2(p) e^{-jp(u-b)} dp,$$

$$r_3(-u) = \frac{R\beta}{2\pi} \int T_1^*(p) T_2(p) e^{-jp(u+b)} dp.$$

The first filtered wavefront  $r_1(-u)$  is centered on the optical axis and is generally of little interest. The second term  $r_2(-u)$  represents the convolution of the two transparencies  $t_1(x)$  and  $t_2(x)$ ; this term is centered at  $u = +b$  and thus separable from the on-axis wavefront. The third term  $r_3(-u)$ , centered at  $u = -b$ , represents the desired correlation between  $t_1(x)$  and  $t_2(x)$ . The coordinates  $u$  in the output plane  $P_3$  have reversed signs as a consequence of the image inversion caused by the spherical lenses; this inversion implies that the filtered image is rotated through 180 degrees, a natural result with any imaging system whether incoherently or coherently illuminated. The positive spherical lenses always introduce a negative kernel function into the Fourier transform operation.

Applying the convolution theorem to the expression for  $r_3(-u)$  and noting that the scale of  $T_2(p)$  is dependent on the separation  $l$  yields

$$r_3(-u) = \int t_1(x+u) t_2\left(\frac{f}{l}x\right) dx.$$

Thus, the output plane  $P_3$  contains the distribution  $r_3(-u)$ , which is the correlation integral of  $t_1(x)$  and  $t_2(\frac{f}{l}x)$ . The scale of the second transparency



can be adjusted to match the reference function  $t_1(x)$  by varying the separation  $l$ .

The capability for scale variation allows the IMF system to use input images that may differ significantly in relative scales. Movement of the image along the optical axis would accomplish image scaling. This feature would be of great importance for the identification and classification of terrain characteristics.

### 3.2 CROSS-CORRELATION PROCESSING FOR PARALLAX MEASUREMENT

A coherent optical correlator is used to determine parallax by cross-correlating small regions in a stereo pair of transparencies. Let us assume that one transparency  $h(x, y)$  from a stereo pair is used to make a spatial filter as described above. The second transparency  $f(x, y)$  and this filter are located respectively in planes  $P_1$  and  $P_2$  of the system shown in Figure 3-1.

If only a small area of the second transparency is illuminated, the output plane  $P_3$  will contain a light intensity pattern corresponding to the cross correlation of this illuminated area with that of the entire first transparency. Ideally, any given small area  $A_h$  will cross correlate strongly with only the corresponding small area  $A_f$  of the first transparency. The position of the cross correlation peak in plane  $P_3$  is fixed by the relative positions of

these two small areas ( $A_h$  and  $A_f$ ) in the input gate. Any change in position for this region between the filter making operation and the cross correlation operation will cause a corresponding displacement shift of the correlation peak in the output plane. This shift in correlation position can be used to measure the parallax between the local regions. By sequentially illuminating portions of the second transparency,  $f(x, y)$ , and detecting the positions of the corresponding correlation peaks, we can measure parallax over the entire input scene.

### 3.3 OPTICAL DATA PROCESSING FOR FEATURE EXTRACTION

Coherent optical processors in general and the IMF breadboard system in particular have considerable potential for feature extraction. The IMF system provides immediate access to a display of the input imagery, the Fourier transform of that imagery, and the parallax information for the stereo pair. The simultaneous presence of these elements in a single system is a unique situation having significant potential for image analysis and feature extraction.

There are three general classes of operations which can be performed directly by a coherent optical system. These are power spectral analysis, simple spatial filtering, and holographic spatial filtering. Additional operations can be implemented by combining the optical processor and a digital

computer. In this hybrid system, data samples provided by the optical system are processed under programmed control by the digital computer; this joint processing capability can perform non-linear operations not easily accomplished with either optical or digital systems separately.

Power spectral analysis is simply accomplished by measuring the intensity distribution in the Fourier transform plane of the processor. A sensor, located in the transform plane would sample the intensity under computer direction. This process could synthesize any desired sampling aperture; discrete, annular, or wedge-shaped samples can be simulated. Significant changes in the power spectra from various local regions of the input imagery can be detected; these changes would outline the regions having certain textural characteristics.

The introduction of various spatial filters into the transform plane can significantly alter the characteristics of an image; either simple or holographic filters can be inserted. Simple filters, such as opaque disks and symmetrical wedges, enhance certain characteristics of the image. This type of image modification technique could be used as a specialized viewing device by a human interpreter. Holographic filters are used to effect a cross-correlation between the input image and a reference scene. This technique can be used to identify and locate specific patterns as well as



provide parallax information. However, the feature of interest must be quite similar in scale and orientation to the reference pattern to produce a significant correlation in the output plane.

## SECTION IV

### CORRELATION DETECTION DEVICES

During the course of the present contract, we investigated the possible application to the ACME system of three different image sensors: a standard vidicon, a charge-coupled device, and a charge-injected device. Each of the candidates utilizes a different technique to produce a video replica of the intensity present in the correlation plane of the processor. In this section, we first review the basic requirements for the output sensor in an automatic stereo compilation system. Next, the image sensors are discussed and their relevant characteristics are given. The section is concluded with a trade-off analysis to establish the device best suited for correlation detection.

#### 4.1 OUTPUT SENSOR REQUIREMENTS

The major function performed in an automatic stereo compilation system is the measurement of ground elevation profiles. Typically, this measurement uses a correlation technique which determines the small parallax displacements of terrain regions in aerial photographs. The correlation technique employed can be one- or two-dimensional in nature. The image matched filter concept used in the ACME system performs a true two-dimensional cross-correlation between the areas of aerial images. During the



parallax collection operation, this cross-correlation is represented by the irradiance distribution in the output plane of the ACME system. The location of the maximum correlation intensity in the output plane provides a measure of the parallax displacement and, hence, the local ground elevation. The level of performance achieved by the system is gauged by the accuracy of the ground elevation values.

A primary burden for the recognition and definition of the peak correlation intensity is placed on the two dimensional area sensor positioned in the output plane. This output sensor, sampling the irradiance distribution in the output plane, provides the conversion from the optical domain to the electronic domain. The conversion must be consistent with overall system requirements.

Several system requirements influence the selection of an output sensor. One set of requirements is presented by the photogrammetric aspects of the parallax data. The parallax values represent the small spatial displacements of terrain areas between two aerial scenes. To provide useful information, the measured parallax values must be referenced to a highly linear, metrically accurate coordinate system. To obtain the degree of precision required, any geometric distortion introduced by the output sensor must be accounted for during the data reduction process. The resolution required

during the parallax measurement is also critical. For typical operational parameters, a difference in actual ground elevation of 0.4 m corresponds to a nominal displacement in the output plane ( $25\text{ }\mu\text{m}$ ); the output sensor must provide resolution on this order.

A separate set of requirements is imposed by the optical detection aspects of the parallax measurements. The intensity of the correlation peak varies significantly as different areas of the image are addressed. The threshold sensitivity of the output sensor must be sufficient to detect the low power signals, while the dynamic range of the sensor must accommodate the intensity variations. The signal-to-noise ratio (SNR) of the output detector is another consideration. Any degradation of the SNR for the optical correlation signal must be minimal. In addition, the SNR of the video correlation signal must be adequate for detection by subsequent processing electronics. The anticipated data collection rate near 30 frames per second also impacts sensor choice. The frame rate fixes the maximum sampling time available to the output sensor. The frame rate and sensitivity of the sensor jointly determine the maximum data collection rates.

Other properties of the sensor must also be considered. The image retention and blooming tendency of the output sensor influence the accuracy of the parallax measurement. Image retention by the output sensor results

from an incomplete erasure of previous images from the sensor area. Image retention by the sensor for an intense correlation peak would degrade the system accuracy for subsequent weaker correlations. Similarly, the blooming tendency of the output sensor can prevent accurate correlation position measurements. Blooming occurs at localized areas of the sensor which receive large overexposures. The blooming causes the apparent size of the affected area to increase; this increased size introduces additional inaccuracies to the correlation measurement process.

#### 4.2 OPERATIONAL PRINCIPLES

In this section, we review the operational principles of three area imaging devices: the silicon vidicon, a charge coupled device (CCD), and a charge injected device (CID). The silicon vidicon, based on a well-established technology, is routinely used for commercial applications. Although vidicon tubes have several desirable features, they do introduce geometric distortion into the scanning process; this distortion is a key consideration for a parallax measurement application. The two solid state arrays, the CCD and CID area imagers, offer excellent metricity. However, these devices do not presently achieve the resolution obtained by electron beam tubes. To establish the limiting performance of the three imaging devices, their basic construction and operation must be considered.



The standard silicon vidicon is an electron tube device which converts an optical image into a video signal. The basic construction and operation of a vidicon relies on a scanning electron beam and a photoconductive target. A transparent conductive layer, coated on the front surface of a photoconductor, acts as a signal electrode. During operation, the photoconductor is initially charged by a scanning electron beam to a uniform surface voltage which creates an electric field within the photoconductive layer. An optical image focused on the photoconductor surface generates charge carriers which migrate under the influence of the applied field to the photoconductor surfaces. These migrating charges modify the original surface voltage present, forming an electrostatic latent image of the optical image. The electron beam, whose size and shape are controlled by focus and deflection coils surrounding the tube, scans in a raster type fashion across the photoconductor and deposits a surface charge in proportion to the local surface voltage. The charge deposition process generates a capacitive displacement current at the signal electrode and returns the surface voltage to its original uniform value. The capacitive displacement current, related to the original optical energy incident on the tube, is used to drive the display and processing electronics.

The charge-coupled imaging device (CCD) represents one technique that achieves the capability of complete solid-state imaging. The CCD

imager is composed of photosensor gates, a vertical line analog shift register, and a horizontal line shift register. The operation of the device is subdivided into three phases: integrate, transfer, and shift. These phases are initiated by the clocked voltage levels present on the photosensor gates, scan gates, and shift registers. During the integrate period, each photosensor of the array is allowed to accumulate a charge packet proportional to the local light energy. A low voltage level on the photosensor gate localizes the charge packet beneath the gate and prevents any charge transfer. During the vertical blanking time, the photogenerated charge packet is transferred into the adjacent CCD shift register element. The charge transfer is enabled by a simultaneous high voltage level on the photosensor gate and a low voltage level on the scan gate. The potential barriers generated by these voltage levels transfer the charge packets into the adjacent elements of the vertical shift register. During the shift phase, each row of the charge array stored in the vertical register is transferred into the horizontal shift register; during this shift phase, the photosites are again allowed to accumulate charge. The horizontal shift register is sequentially clocked to produce the video replica of the original image.

The charge-injected imaging device (CID) represents an alternative technology for solid state imaging systems. The basic operation of the CID is similar to that of the CCD. The CID operation is also divided into three

phases: integrate, transfer, and inject. As in the CCD technology, these phases are initiated by clocked voltage levels on the photosensor and transfer gates. During the integrate phase the photosensor sites are allowed to accumulate a charge packet corresponding to the incident light intensity. When one row of the array is selected for readout, the charge packet is transferred to the adjacent charge storage elements. The transfer is initiated for a particular photosite by a simultaneous high voltage level on the photogate and low voltage level on the transfer gate. A selection circuit for the CID sequentially transfer the charge packets from the photosensor area to the storage areas. Although normally operated in this sequential mode, the CID does possess the capability for random access addressing. The charge packet stored at each site is sensed by injection into the bulk silicon substrate and detection of the associated displacement current. An on-chip amplifier converts the displacement current into a video replica of the original image.

#### 4.3 DEVICE TRADE - OFF ANALYSIS AND SELECTION

The relative performance levels achieved by the three types of imaging devices are summarized in Table 4-1. The devices summarized in the table are commercially available and are generally representative of their respective technologies. The vidicon, an MTI Type V-440, provides a



Table 4-1 Typical Performance Parameters for Vidicon, CCD and CID Imaging Devices

Parameter	Unit	Imaging Device		
		625 Line Vidicon	244 x 190 Element CCD Area Sensor	244 x 188 Element CID Area Sensor
Scan Nonlinearity	%	1	< 0.1	< 0.1
Geometric Distortion	%	2	< 0.1	< 0.1
Resolution at 50% Response	cy/mm	18	10	10
Saturation Exposure	fcs	0.02	0.004	0.03
Maximum Signal-to-Noise Ratio	dB	30	25	30
Dynamic Range		500	300	500
Image Retention (3rd Field)	%	15	< 0.1	< 0.1

scanning rate for 625 TV lines of 30 frames per second. The CCD imaging device, a Fairchild CCD-211, provides scanning of 488 video lines at rates up to 100 frames per second. The CID imaging device, incorporated in the General Electric Z7892 CID television camera, provides a resolution of 488 video lines at a 30 frames per second scan rate. Both solid state devices utilize a multiplexing technique to achieve their full resolution.

The non-linearity and geometric distortion are significantly higher for the vidicon than for the solid state sensors. The predominant cause for this effect is the deflection system employed in the vidicon. Typically, pincushion distortion is the main aberration causing the nonlinearity. The use of a parabolic sweep generator and precision deflection yokes for the vidicon can reduce the pincushion distortion significantly; however, the high scan fidelity is attained only with the sacrifice of deflection speed and an increase in device cost. The linearity and distortion levels achieved for the solid state sensors is completely dependent on fabrication techniques. In addition, the presence of extraneous magnetic fields does not compromise the performance levels for the solid state sensors.

The resolution achieved by vidicons is higher than that of current solid state sensors. The resolution for the vidicon is limited by the bandwidth of the focussing coil and camera chain. The size of the scanning electron beam is fixed by the focussing coil. Whereas the time response is determined by bandwidth constraints. Present state-of-the-art vidicons are

limited to a maximum resolution of 2000 lines at TV frame rates. Presently, solid state sensors do not achieve this resolution. Typical resolutions achieved with the solid state devices are half that of standard vidicons. However, the resolution of available CCD and CID arrays will improve as fabrication experience and techniques are developed.

The sensitivity, signal-to-noise- ratio, and dynamic range are also important system considerations. These parameters establish the operating characteristics of the image sensor. The sensitivities listed in Table 4-1 are for particular devices and are not indicative of fundamental technology limitations; sensors are available which function in ambient light levels of  $10^{-6}$  footcandles. The vidicon and CID presently have sensitivities in the range necessary for the ACME system. The higher sensitivity provided by the CCD imager would necessitate added attenuation in the optical system. Precautions to ensure no stray light degradation would also be necessary. The signal-to-noise ratio and dynamic range provided by the sensors are consistent with correlation recognition and detection.

Image retention or lag by the output sensor is another practical consideration. Image lag by the output sensor allows a signal, although attenuated, to persist for several video frames after its initial occurrence.



The image lag properties of the solid state devices are superior to those of the vidicon. Image retention of the vidicon results from an incomplete erasure of the photo-induced surface voltage. The amount of retention is dependent on signal level; the table listing is representative of the retention for an average signal level. Image retention in the solid state devices is caused by an incomplete transfer of charge from the photosites. A typical level of the transfer inefficiency averaged over a video frame is  $0.5 \times 10^{-4}$ . No degradation is caused by transfer inefficiency for solid state arrays with element densities in the range anticipated.

The high metric fidelity required for the stereo compilation system is presently achieved only by the solid state imaging arrays. To achieve the same level with a vidicon would require a substantial increase in both device complexity and expense. Similar limitations exist for increasing the frame rate capability of the vidicon; special yoke and electronic design are required to achieve faster frame rates. These limitations eliminate the vidicon as a viable candidate for a stereo compilation system.

The two remaining candidates, the CCD and CID area imagers, have comparable performance. Of these two, the CID area imager is easier to fabricate. This typically yields CID imagers with fewer blemishes or bad sites than comparable CCD devices. The readout process for the CID is

slightly noisier than that for the CCD; the increased noise arises from the higher output capacitance of the CID area imager. However, an acceptable SNR can be achieved with both devices. The readout stream from the CCD is necessarily serial in nature; the CID can be addressed in an x-y matrix fashion. Thus, the CID has a capability for random access readout. The random access feature is desirable for an application such as stereo compilation. The random access ability of the CID supports fast readout rates while still providing metric accuracy. As the technology for charge injection devices matures, it is reasonable to expect that even higher resolution (over 1000 elements per axis) can be achieved. The CID area imager, with its random access capability, is the preferred detector for an engineering model stereo compilation system.

## SECTION V

### IMF SYSTEM CONFIGURATION

A major goal of this contract was to develop and refine techniques for the automatic extraction of parallax data from aerial photographs. In particular, a hybrid electro-optical system capable of collecting parallax data at rates of 30 samples per second was implemented. In this section of the report we present a functional description of this system concept. The description details the optical and electronic subsystems involved and covers the control functions provided by software. The section is concluded by a discussion of the development, results and status of the present experimental system.

#### 5.1 IMF SYSTEM DESCRIPTION

Cross correlation techniques are used in the Image Matched Filter (IMF) system to measure terrain profile. The cross-correlation operation, giving the best linear estimate of similarity, is dependent on the relative displacements between the two functions evaluated. Thus, the position of the cross-correlation peak gives a direct measure of the relative displacement, or parallax.

A key end use identified for the IMF system is the fast and accurate measurement of this parallax. The measurement process involves deter-



mining small, typically 50 to 100  $\mu\text{m}$ , displacements in the relative position of a terrain region in two separate aerial photographs. The parallax measurement must be performed at 0.5 mm intervals over the photographs forming the stereo pair.

Several key subsystems are required in the IMF system for the parallax measurement process. An optical subsystem must be assembled to perform a cross-correlation between two functions contained in transparency form; a Fourier transform geometry is employed to cross-correlate one entire scene, stored as an image matched filter, and a small localized region of the second scene. An electronic subsystem must provide the necessary functions to operate the system; these functions include accessing a specified location in the second scene and determining the position and intensity of the correlation peak. The overall timing and control for operation and the actual data collection and storage must be accomplished by a programmable control unit which monitors the process.

The interrelationships and functions of these subsystems are shown by the block diagram in Figure 5-1. Under software control the programmable control unit (PCU) selects a specified location in the second transparency at which parallax is to be measured. Binary values corresponding to this physical location are routed to digital-to-analog converters (D/A); the

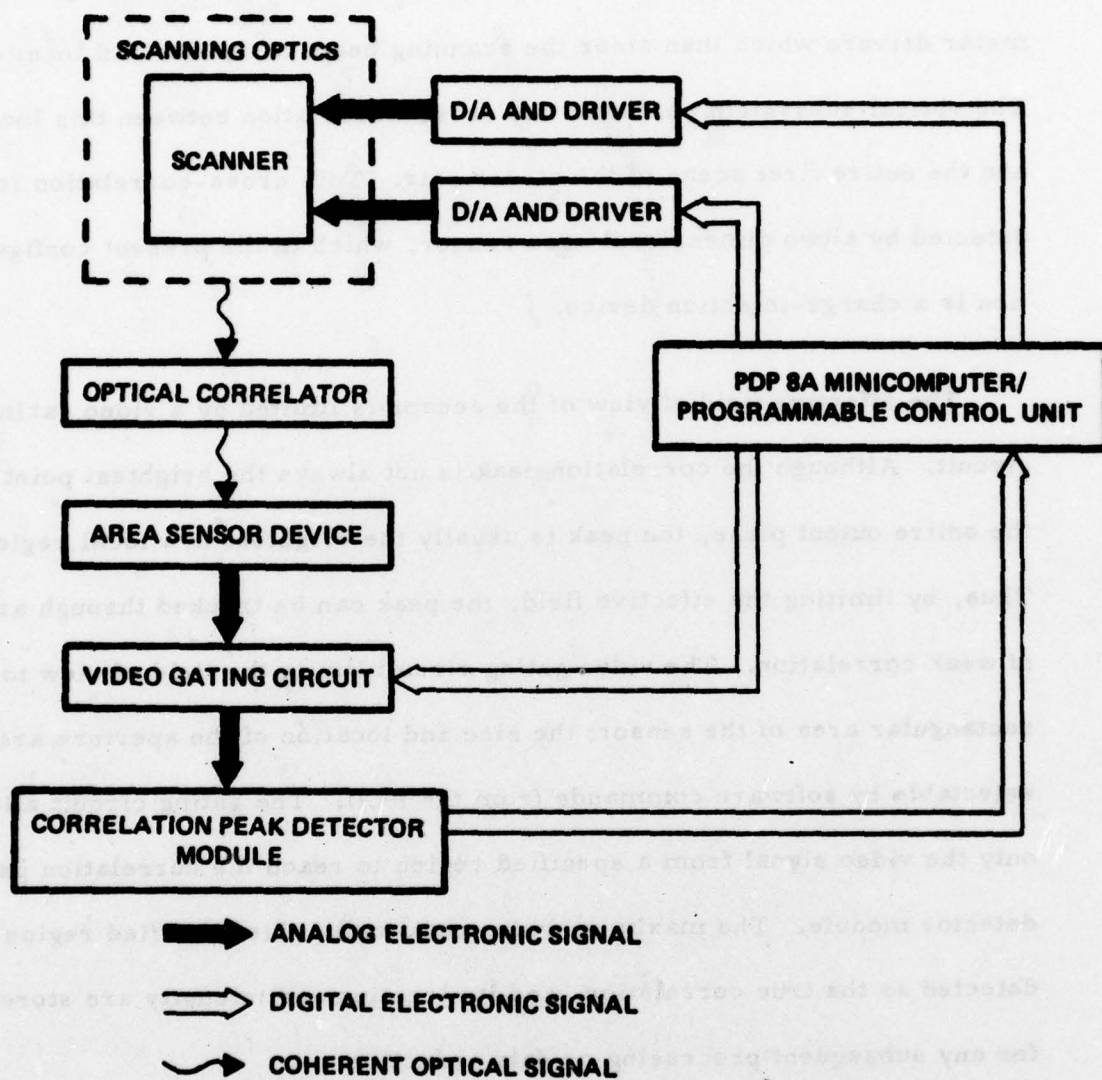


Figure 5-1 Functional Schematic of the IMF System

D/A units convert the binary signal into an analog voltage for the galvanometer drivers which then steer the scanning beam to the desired location. The optical subsystem performs the cross-correlation between this location and the entire first scene of the stereo pair. This cross-correlation is detected by a two dimensional area sensor, which in the present configuration is a charge-injection device.

The effective field of view of the sensor is limited by a video gating circuit. Although the correlation peak is not always the brightest point in the entire output plane, the peak is usually the brightest in a local region. Thus, by limiting the effective field, the peak can be tracked through areas of weak correlation. The video gating circuit limits the field of view to a rectangular area of the sensor; the size and location of the aperture are selectable by software commands from the PCU. The gating circuit allows only the video signal from a specified region to reach the correlation peak detector module. The maximum video peak within this specified region is detected as the true correlation, and its location and intensity are stored for any subsequent processing or data reduction.

At this point the parallax values for one specified location have been established and stored. Depending on the stage of program completion, another scan point can be selected for parallax measurement or a data re-



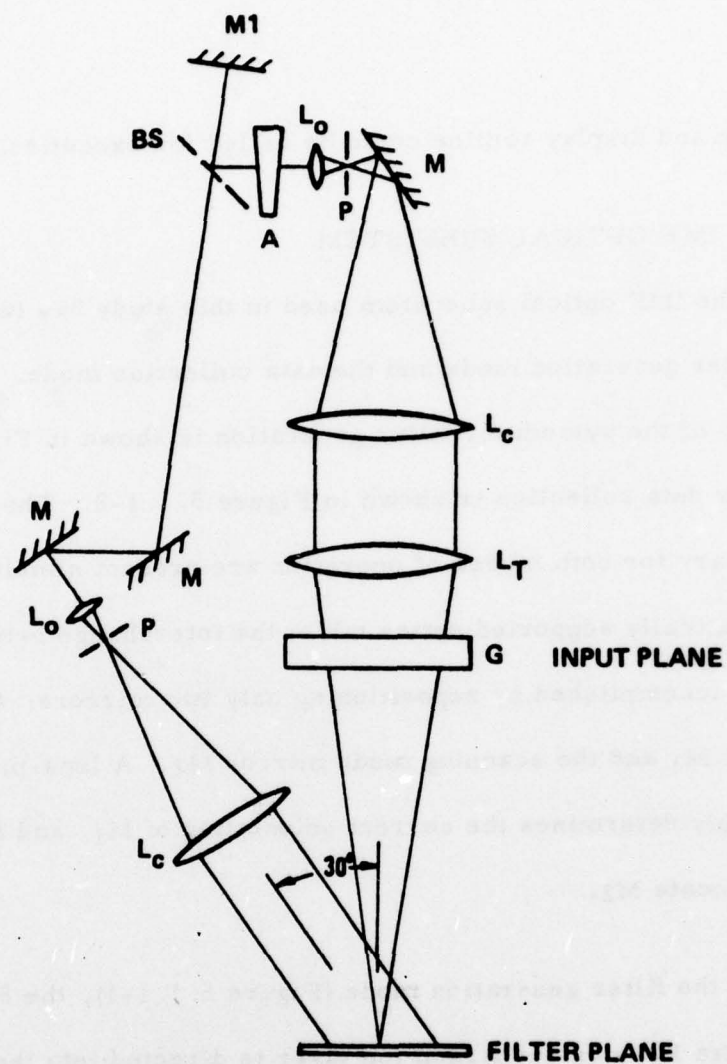
duction and display routine could be called for execution.

#### 5.1.1 IMF OPTICAL SUBSYSTEM

The IMF optical subsystem used in this study has two functional modes: the filter generation mode and the data collection mode. The present configuration of the system for filter generation is shown in Figure 5.1.1-1, and that for data collection is shown in Figure 5.1.1-2. The components necessary for both modes of operation are present simultaneously on the pneumatically supported optics table; the interchange between modes is easily accomplished by repositioning only two mirrors: the beam routing mirror  $M_1$  and the scanning mode mirror  $M_2$ . A lens-pinhole spatial filter assembly determines the correct orientation of  $M_1$ , and fixed mechanical stops locate  $M_2$ .

In the filter generation mode (Figure 5.1.1-1), the 514.5 nm light from a Spectra Physics 165 Argon ion laser is directed into the system by beam routing mirror  $M_1$ . The incident laser beam is split into a signal and a reference beam by a beamsplitter. The reference beam is then spatially filtered and collimated with its axis at an angle of  $30^\circ$  to the signal beam axis.

The signal beam forms a point source at P which is imaged into fil-



- |   |                                   |
|---|-----------------------------------|
| M1 - BEAM ROUTING MIRROR                | M - MIRROR                        |
| BS - BEAM SPLITTER                      | G - LIQUID GATE                   |
| A - ADJUSTABLE ATTENUATOR               | L <sub>c</sub> - COLLIMATING LENS |
| L <sub>o</sub> - MICROSCOPE OBJECTIVE   | P - PINHOLE                       |
| L <sub>T</sub> - FOURIER TRANSFORM LENS |                                   |

Figure 5.1.1-1 IMF Optical Subsystem: Filter Generation Mode

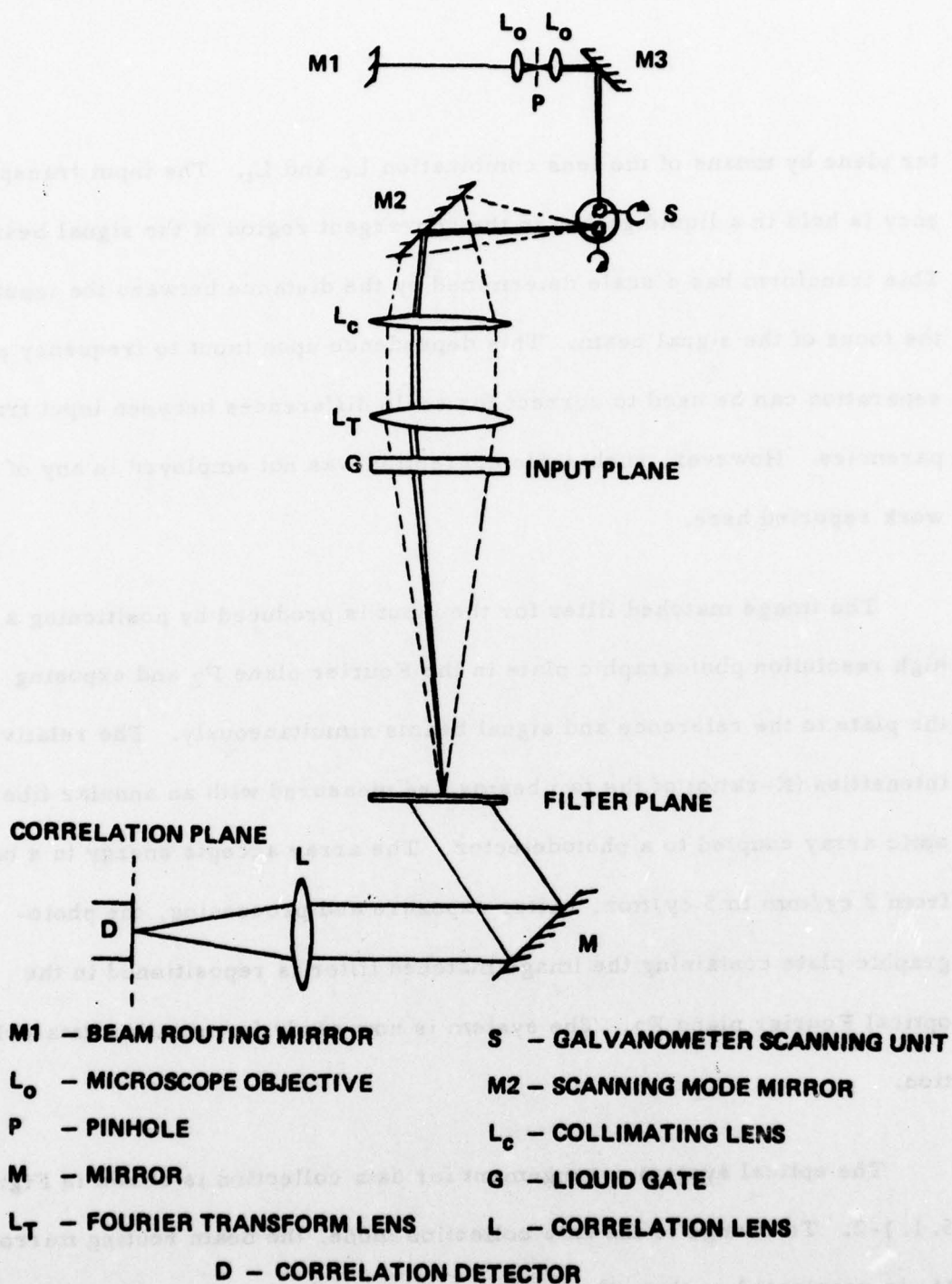


Figure 5.1.1-2 IMF Optical Subsystem - Data Collection Mode



ter plane by means of the lens combination  $L_c$  and  $L_t$ . The input transparency is held in a liquid gate G in the convergent region of the signal beam. This transform has a scale determined by the distance between the input and the focus of the signal beam. This dependence upon input to frequency plane separation can be used to correct for scale differences between input transparencies. However, such scale correction was not employed in any of the work reported here.

The image matched filter for the input is produced by positioning a high resolution photographic plate in the Fourier plane  $P_2$  and exposing the plate to the reference and signal beams simultaneously. The relative intensities (K-ratio) of the two beams are measured with an annular fiber optic array coupled to a photodetector. The array accepts energy in a band from 2 cy/mm to 5 cy/mm. After exposure and processing, the photographic plate containing the image matched filter is repositioned in the optical Fourier plane  $P_2$ . The system is now ready for parallax data collection.

The optical system arrangement for data collection is shown in Figure 5.1.1-2. To change to the data collection mode, the beam routing mirror  $M_1$  is reoriented so that all of the laser light is directed to a telecentric galvanometer scanner. The beam in this case is formed in a narrow cone

which illuminates an area approximately 1 mm in diameter at the input gate. The scanning beam routing mirror  $M_2$  is translated into position against fixed stops when converting to the data collection mode.

The telecentric scanner consists of two small galvanometers whose axes are at right angles and whose mirrors are in the conjugate planes of a folded telescope. The scanner is positioned so that the scanning beam pinhole is imaged onto the center of both mirrors. This assures that the scanning beam always appears to come from the same point regardless of the direction in which it is deflected. The scanner and scanning beam optics are arranged so that the scanning beam pinhole and the telecentric scanner are optically at the same position with respect to the lens pair  $L_c$  and  $L_t$  as the signal beam pinhole was during filter generation. When the system is properly aligned, the image of the scanning beam pinhole remains stationary regardless of the position of the scanning beam in the input gate.

The image matched filter, when illuminated by a wavefront derived from a corresponding area of the input transparency, reconstructs a modified version of the original reference beam at a nominal angle of  $30^\circ$  to the optical axis. This beam is reflected by the mirror to the lens  $L$  which forms the cross correlations in the output (correlation) plane. This lens and mirror are mounted on a small auxiliary optical rail attached to the top

of the optical table.

The cross-correlation is detected by a two-dimensional area sensor, which in the present configuration is a charge injection imaging device. The camera converts the optical signal into an electronic video signal for subsequent processing and correlation detection.

Additionally, a two dimensional fiber optic array is mounted on the input gate. This array consists of a horizontal and vertical row of fibers positioned along two adjacent edges of the input gate. These fibers lead to a single photodetector whose output is sensed by an A/D converter interfaced to the programmable control unit. By moving the scanning beam along this array, the PCU can automatically calibrate and linearize the galvanometer scanner.

#### 5.1.2. IMF ELECTRONIC SUBSYSTEM

The automatic recognition and detection of the correlation peak involves a number of operations. First, the correct correlation peak must be identified. Although this operation is relatively straightforward for regions of high signal-to-noise ratio (SNR) and adequate intensity, it is generally not possible on a global basis. The correlation peak typically has a high localized SNR, but is not the most intense point in the entire output plane.



Thus, the effective field of view for the sensor must be limited in regions of weak correlation. In addition, the position of this limited field of view must be controlled by software commands to track the changing correlation function. Second, the correlation peak location must be measured with high precision. This measurement process must be consistent with high speed processing, while not requiring excessive bandwidths. Third, the technique should be compatible with several output detector types, including standard vidicon imaging tubes and solid state arrays.

Other functions must be provided by the electronic subsystem. The interface must provide the drive signals for scanner operation; the drive signals should be compatible with software control to correct for changes such as scene orientation or scale drifts. The electronics must also measure the intensity of the correlation peak. The intensity is useful in establishing the field of view for the sensor. In addition, this feature can provide a means to sample and quantize an arbitrary intensity distribution; this capability could be applied to power spectral analysis.

We developed a correlation peak tracking technique using these above considerations as design goals. The technique is based on the use of a peak stretching circuit in conjunction with a clock and counter. The peak stretching circuit determines the most intense point contained in the video signal;

the clock and counter define the location of this point. A video gating circuit is added to the peak detection module to allow only a selected area of the output plane to be processed.

The functional schematic of the IMF electronic subsystem is shown in Figure 5.1.2-1. The programmable control unit (PCU), a Digital Equipment Corporation PDP - 8A minicomputer, provides the central direction for the parallax data collection process. Under software control the PCU establishes the boundaries of the rectangular region of the output plane selected for processing. These boundaries are defined by four digital words which designate the TV line numbers and times along these lines which limit the field of view. These words are loaded into the buffers of the aperture location module and are retained until updated. These buffers control the start and stop action of a gated amplifier in the sync removal and video gating circuit. The input to the amplifier is the composite video signal from the camera which is located in the correlation plane. The horizontal and vertical sync signals from the camera drive a frame synchronous clock which runs at 200 times the TV line rate; this clock is used to measure time along a scan line. Digital comparitors in the video gating circuit monitor the values of the frame synchronous clock and TV line number. When these values are within the range specified by the aperture location module, the composite video signal is gated through to the peak detector.

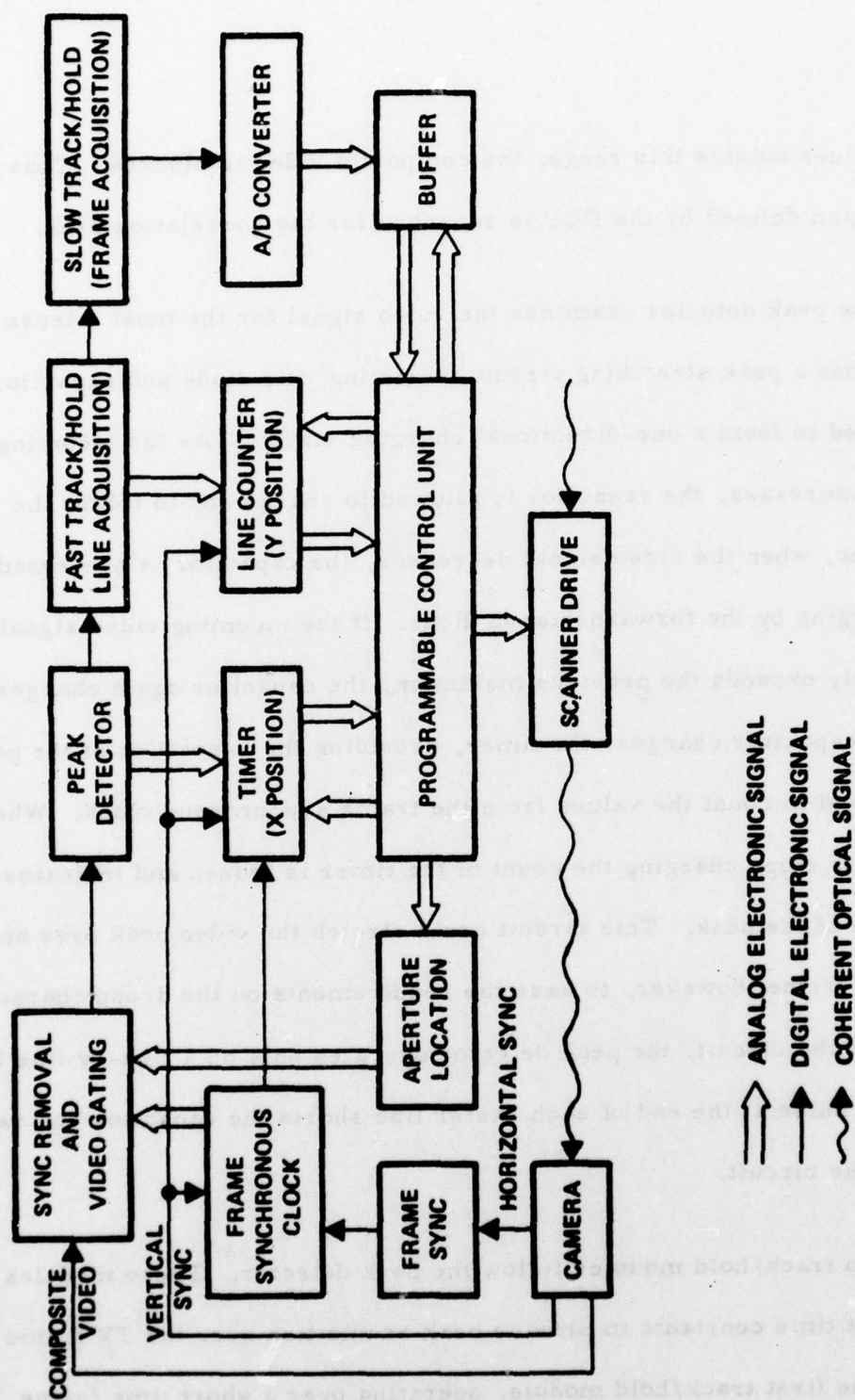


Figure 5.1.2-1 Functional Schematic of the IMF Electronic Subsystem



For values outside this range, the composite video is blocked. Thus, only the region defined by the PCU is searched for the correlation peak.

The peak detector examines the video signal for the most intense point with a peak stretching circuit consisting of a diode and capacitor arranged to form a one-directional charging circuit. As the incoming video signal increases, the capacitor is allowed to charge and to follow the input. However, when the video signal decreases, the capacitor is prevented from discharging by the forward-biased diode. If the incoming video signal subsequently exceeds the previous maximum, the capacitor again charges. As the capacitor charges, the timer, providing the x-position of the peak, is allowed to count the values from the frame synchronous clock. When the capacitor stops charging the count of the timer is frozen and indicates the position of the peak. This circuit could stretch the video peak over an entire TV frame; however, to ease the requirements on the droop characteristics of the circuit, the peak detector operates only on a line-by-line basis. A reset pulse at the end of each raster line shorts the capacitor and reinitializes the circuit.

Two track/hold modules follow the peak detector. These modules have different time constants to provide peak acquisition over the TV frame period. The first track/hold module, operating over a short time frame,

acquires the peak values for contiguous lines and compares them to determine the maximum value. Each time a maximum peak is encountered, the line counter is loaded with the corresponding line number. At the conclusion of a frame the timer and line counter contain the values corresponding to the peak location.

The second track/hold module follows the peak value over the time interval specified by the contents of the aperture location buffers. At the conclusion of the frame, the peak intensity held by the second track/hold module is converted into a digital word and loaded into a buffer. The PCU by polling the timer, line counter, and buffer can establish the x-position, y-position, and intensity of the correlation peak. The PCU stores these values and selects the next scan location. The aperture location is updated and the process is repeated for the new scan location.

The schematics for the circuits implemented for the IMF system are presented in Appendix A. The appendix details the computer interface circuits, the aperture location module, and the track/hold circuits. In addition, the analog electronic circuit which performs the peak detection is included.

The analog detection module was first fabricated using a vector board construction. Initial testing of this module revealed a noise problem caused

by low signal levels and incomplete component isolation. To remedy this situation, the analog detection module was subsequently fabricated on a copper-clad printed circuit board which provided a positive ground plane and increased noise isolation. Preliminary tests of this module showed improved noise performance in a static testing mode. The digital interface circuits were fabricated on standard Digital Equipment Corporation cards and installed in the programmable control unit. Complete details of the interface performance are given in Section 5.2 of this report.

#### 5.1.3 IMF SOFTWARE CONTROL FUNCTIONS

The control functions for the IMF system are provided by the programmable control unit through software routines. The programmable control unit is a Digital Equipment Corporation PDP-8A minicomputer with 32k words of on-line storage capacity and dual floppy disc drive units for off-line storage. The major controlling programs are written in FORTRAN-II, a high level language chosen for its rapid execution times. Support programs and subroutines utilize SABR<sup>R</sup>, a language commonly used on the PDP family of minicomputers from Digital Equipment Corporation. These two languages were selected for use because of their relative programming simplicity. Device handlers providing control over external equipment can be developed in the SABR language; the SABR handlers can subsequently be used directly by the main FORTRAN-II calling program.



Interface options are available on the IMF system to support computer control of all major operations including the linearization and calibration of the galvanometer scanner, the drive and control of the galvanometer scanner, and the automatic collection of parallax data for stereocompilation. During previous contractual phases, the scanner linearization feature has been demonstrated. During the present effort, this capability was not employed; however, the hardware components and interface ports are available in the present system.

The scanner linearization can be accomplished by utilizing the fiber optic array located at the periphery of the input liquid gate. The L-shaped array consists of 250  $\mu$ m diameter optical fibers spaced on 5.00 mm centers; the fiber array, terminated at a common photodetector, does not block the active scan region of the gate. To linearize the scanner, the operator initially directs the scanning beam to the corner fiber of the array. Under programmed control the beam is incrementally stepped across the horizontal and vertical legs of the array. At each position of the beam, an A/D conversion of the photodetector output can be performed. By locating the positions that correspond to maximum transmitted power levels, the computer can develop an array of digital values corresponding to known

<sup>R</sup> Trademark of Digital Equipment Corporation.

physical locations. This data can be stored and used to linearize the scanning system. In order to calibrate these parameters in terms of direct photocordinates, the operator must direct the scanning beam to several reseau in the input scene. Software developed during previous contractual phases can perform the necessary transformation from the fiber optic array coordinates to the input photocordinates; this transformation accounts for scale changes as well as rotations.

The control of the scanning system is provided by two digital-to-analog (D/A) converters in the computer interface. Binary values corresponding to given physical locations are sent to the D/A converters; these values are subsequently converted to analog levels which are supplied to the galvanometer drivers. Computer controlled operation of the scanning system was demonstrated on earlier program phases where its accuracy and value was proven. A separate interface compatible with the programmable control unit and different software device handlers consistent with the new operating system were developed to utilize the automatic scanning process.

The package for automatic parallax collection was similarly developed; this package contained the electronics required for video gating and peak detection, as well as the circuitry for reading the correlation position and intensity. The software required to provide the timing and control of the

interface electronics was also developed for the new PCU. This software package also provides the internal storage and a video storage of the collected data.

The flowchart indicating the operation of the data collection program is shown in Figure 5.1.3; a complete program listing is contained in Appendix B. Correct operation requires that the scanning sequence is initialized. This off-line, manual operation involves the adjustment of input scene orientation and the selection of  $N_1$ , the number of data samples per parallax point. The scene orientation is checked by comparing the projected image of the input scene with the reconstructed image of the reference scene. The number of data samples per parallax point is specified in response to computer prompting and represents the number of consecutive video frames over which the correlation peak is averaged.

After the scanning sequence has been initialized, the computer directs the scanning beam to the first point at which parallax data is to be collected. The correlation peak, indicating the parallax values for this initial point, is displayed on the video monitor along with a pair of electronically generated crosshairs. The operator identifies the location of the peak and enters a series of change values until the crosshairs and peak are coincident. This operation establishes the first correlation peak for the computer; the auto-



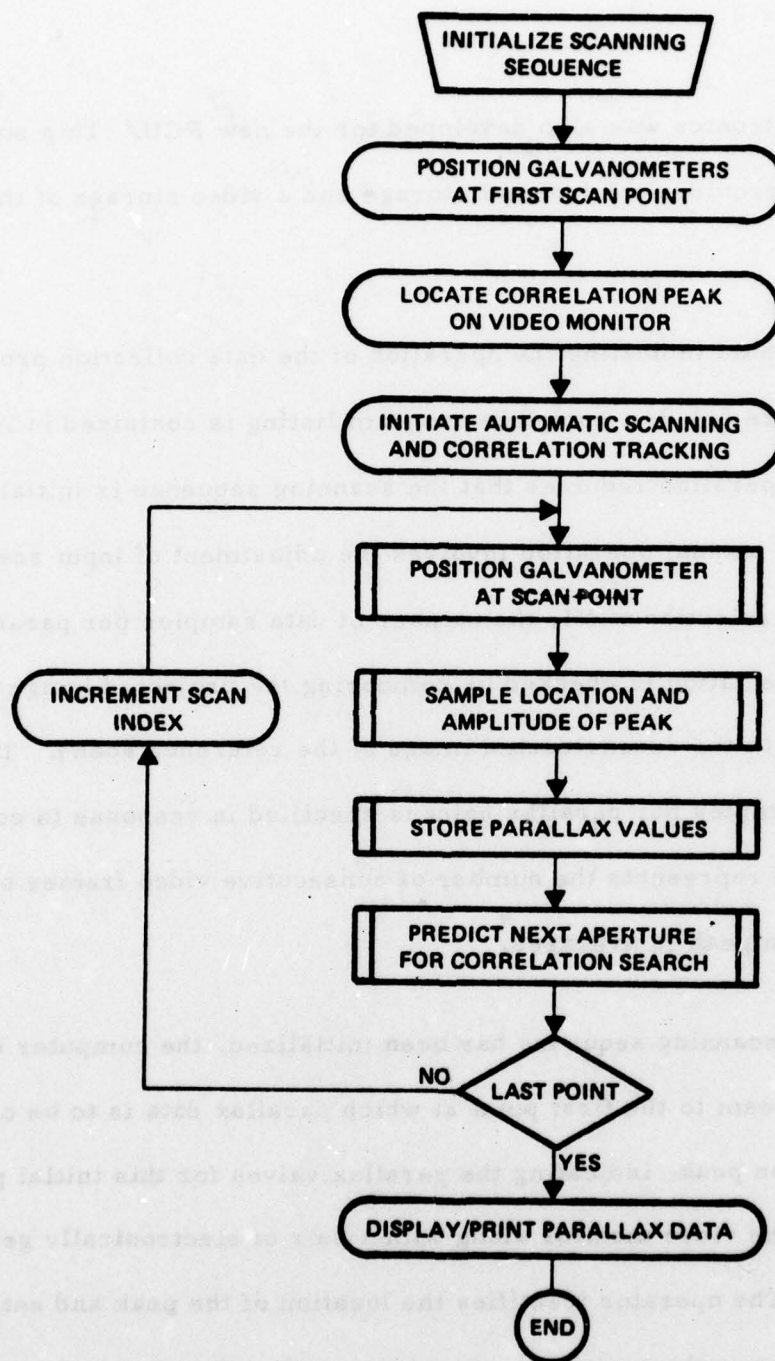


Figure 5.1.3 Flowchart for Software Program Operation

matic data collection process now begins.

The scanning beam is directed to the next point. The location of a fixed aperture region, representing approximately 1 per cent of the sensors field of view, is simultaneously displayed on the video monitor. This aperture determines the region of the active video frame examined for the correlation. The interface electronics search this region for the most intense point and store its location and amplitude in a series of buffers. When the end of the aperture has been reached, a flag is set. The computers, sensing this flag, reads and subsequently stores the contents of the buffers. This search and store sequence is repeated as required by the valve N1. The series of values determined for the point are appropriately averaged and entered into the array of parallax valves. Based on the last locations of the correlation peak, the location of the aperture for the next scan point are then collected using this predicted aperture location.

The data collection process is repeated until the last scan point has been reached. The programmable control unit then display the parallax data collected for the scan. Two types of display are used; a video display is provided, as well as a point out. The electronic crosshairs are directed to trace the profile defined by the correlation peak during the scan; this trace is displayed on the video monitor. The array of valves representing

the horizontal and vertical locations and the correlation intensity are printed on the output terminal; the values can be used for further analysis or data collection.

The software program controlling the data collection process has five major subroutines. These subroutines direct or control a specific portion of the overall process. The GALVO subroutine controls the values output to the scanning system; the subroutine accepts two digital values, directs the digital-to-analog conversions, and routes these analog values to the galvanometer drivers. The AP subroutine controls the location and size of the electronic aperture. The AP subroutine accepts four arguments which represent the locations of crosshairs on the video monitor and define the active search region for the peak detection electronics; the subroutine checks the bounds on these arguments and injects them into the video signal. The remaining three subroutines provide the actual correlation peak acquisition. The PEAK subroutine reads the contents of the buffers holding the horizontal location, vertical location, and intensity of the correlation peak.

The subroutine also provides the timing and control to ensure synchronism of the scanning process with the video detector. The PEAK routine calls the two additional subroutines, ADC and CRVT, to support the interface read operation. The ADC routine directs an analog to digital conver-



sion of the peak intensity, whereas the CRVT routine masks unnecessary bits from the two location registers.

## 5.2 IMF SYSTEM: DEVELOPMENT RESULTS AND STATUS

During the past and present contractual phases, the concepts and techniques developed for the IMF system have demonstrated the applicability of coherent optical processing to the stereocompilation problem. One particular area in which a significant improvement in correlation has been obtained is the preprocessing of input imagery. The edge detail contrast of an aerial photograph is one of the most important factors affecting correlation performance in both coherently and incoherently illuminated optical systems; images having greater edge detail contrast typically produce correlation peaks with a higher signal-to-noise ratio than do images with lower contrast. High contrast regions have more energy in the spatial frequency bands critical to matched filter correlation and scatter less noise from the film grain.

Two techniques were examined which demonstrated successful edge enhancement. Silver-masked input scenes prepared manually and input scenes prepared on automatic dodging contact printing equipment showed an improvement in correlation performance in comparison to standard contact points onto high contrast emulsions. In the "silver masking" technique,

a silver mask is formed by printing the original diapositive aerial photograph onto a low contrast, negative working film. The original photograph is then placed in contact with an unexposed photographic plate having a high contrast emulsion. The silver mask is placed on top of the diapositive. During exposure, the diapositive forms a sharp positive image on the unexposed plate, while the silver mask casts a blurred negative image. On a gross scale, the transmissions of the original and the mask tend to cancel and produce a nearly uniform exposure; however, on a smaller scale, the sharp edge detail of the diapositive is retained, since the mask produces a blurred image. However, gross tonal variations are smoothed in the high contrast copy, and high edge contrast is maintained throughout.

The automatic dodging contact printer also provides edge enhanced imagery with gross tonal variations removed. The automatic printer uses a CRT as a light source with additional exposure control circuitry. The scanning spot of the CRT is projected onto the plane containing the image to be copied and the copy material. A photomultiplier tube (PMT) is used to monitor the transmitted light from the CRT through the image. The PMT output signal, a measure of local density, is used to increase or decrease the velocity of the scanning spot. As the scanning spot is swept in a raster pattern across the input scene, the copy material receives varying point-

to-point exposure determined by local density values. The amount of edge enhancement in the resulting image is determined by the size of the scanning spot and contrast of the copy material.

Although the silver masking technique ultimately offers a greater improvement in correlation performance, the dodging contact printer can be adapted to automatic operation. In addition, further modifications to the automatic dodging process are possible which can provide nearly equivalent performance. These results are also applicable to electronic correlation, such as the AS-11 stereocompilation system.

The accuracy and precision provided by coherent optical processing techniques have also been demonstrated. Parallax data collected on the IMF system was reduced and compared to similar data collected on the Bendix AS-11 system. The data reduction accounted for the scale change, as well as the rotational and translational biases present in the data. The data sets obtained are shown in Figure 5.2-1. The parallax data obtained with both systems for a section of the Canadian Test Model are in good agreement. The root mean square difference between data sets is approximately  $25 \mu m$  if the small region (located near 14 mm) at the edge of a precipitous cliff is ignored. (The position of the cliff varies rapidly and a slight displacement between the IMF and AS-11 scan paths can introduce



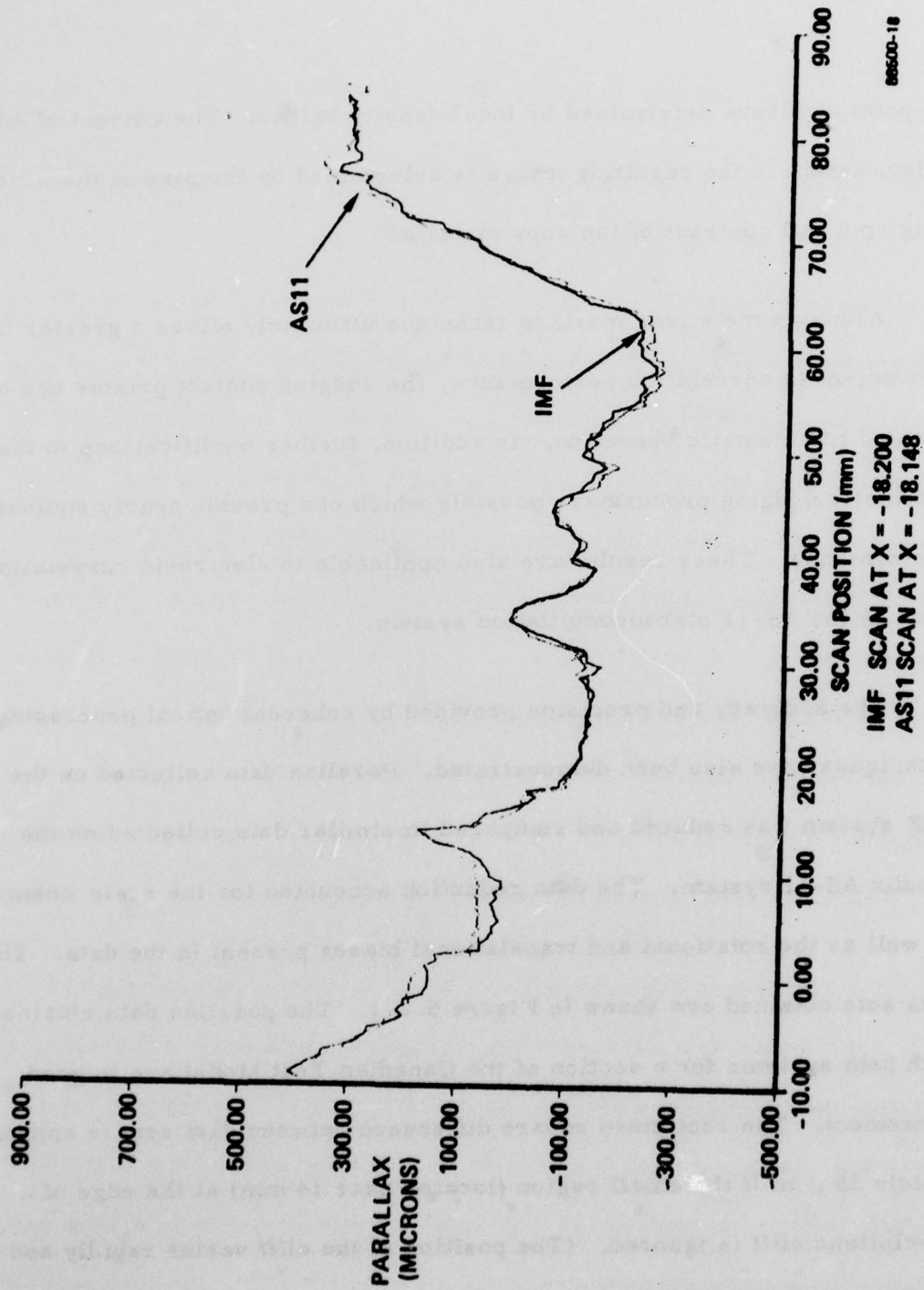


Figure 5.2-1 IMF and AS11 Parallax Data for Canadian Test Model

large parallax changes). For typical operational parameters, this parallax difference corresponds to a ground profile uncertainty of 0.4 m. Considering the hardware limitations of the present developmental system, these results show remarkable accuracy and demonstrate the feasibility of employing coherent optical techniques for stereocompilation.

Methods for improving the accuracy of the IMF system have also been examined. In particular, the performance of the scanning system has been investigated. A major result is the improvement in beam pointing accuracy achievable with a closed loop, temperature regulated galvanometer. This galvanometer type exhibited a pointing accuracy approximately five times more precise than that of the corresponding open-loop devices currently used in the system. Over a three hour observation period, the angular drift of the open-loop galvanometer was typically 1.5 mrad, corresponding to a positioning error of 900  $\mu$  m. The stability of the closed-loop, temperature regulated galvanometers was considerably better; the rms error in pointing accuracy over a two hour period was 0.26 mrad. The residual errors of the closed loop galvanometers can be corrected with optical feedback techniques.<sup>2</sup> The current phase of system development has been primarily concerned with three areas: the identification of a solid state imaging device for correlation detection, the implementation of an electronic interface for automatic correlation location, and the development of soft-

ware for parallax collection at 30 samples per second.

Three different imaging devices were evaluated as possible output detectors: a standard silicon vidicon, a charge-coupled device, and a charge injection device. A description of their operation and the details of their performance are given in Section IV of this report. The charge injection device was the candidate detector selected for the IMF system. A CID camera system was procured and subsequently installed in the breadboard. To account for the lower sensitivity of the CID in comparison with the previous vidicon camera, bleached phase matched filters were used for correlation. These filters allowed a significant increase in diffracted energy without a decrease in signal-to-noise ratio; the average intensity provided by the bleached filters to form the correlation was sufficient for the CID camera. The solid state imaging device also exhibited lower video noise levels than the conventional electron beam imaging tubes examined.

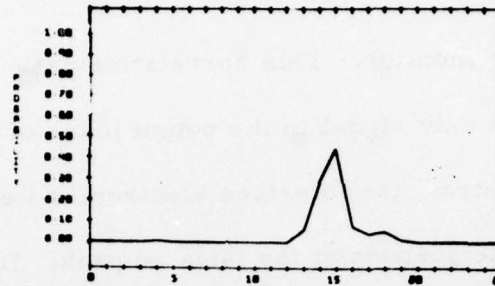
An electronic interface providing the required processing and control functions for automatic correlation peak detection was assembled. This interface system, described in Section 5.1.2, is compatible with both the CID solid state array and conventional vidicon-type devices. The accuracy and precision obtained with the interface were evaluated in both static and dynamic modes. For the static mode tests, a correlation peak was dis-



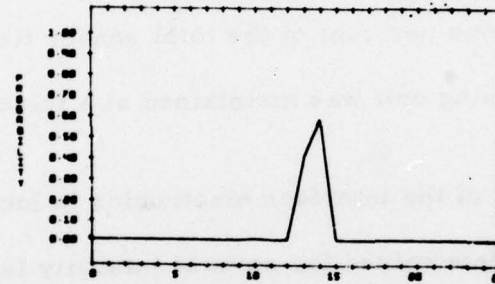
played on the video monitor. This correlation peak had an adjustable intensity and was the only signal in the output plane of the optical processor. Under software control, the interface electronics were directed to repeatedly acquire the position of the isolated peak. During this process, the aperture which restricts the sensor field-of-view was fixed and represented approximately one per cent of the total sensor field. Similarly, the galvanometer scanning unit was maintained at a fixed location.

The accuracy of the interface electronics in locating the defined correlation peak was determined for several intensity levels ranging from a visually detectable level of 25 mV to an intense correlation peak of 200 mV. The results of these static mode tests were analyzed and subsequently graphed in histogram form. These histograms are shown in Figures 5.2-2 through 5.2-4. The histograms show the frequency of position occurrence as a function of position; the positions have been normalized to span a fifteen unit interval. Each unit represents a single position movement. In the vertical direction, the increment represents one clock count. In the spatial domain, both of these units correspond to a nominal  $25\mu$  m displacement. Examination of the histograms show that, although the positional accuracy of the interface electronics is dependent on signal intensity, acceptable performance is obtained in the static mode.

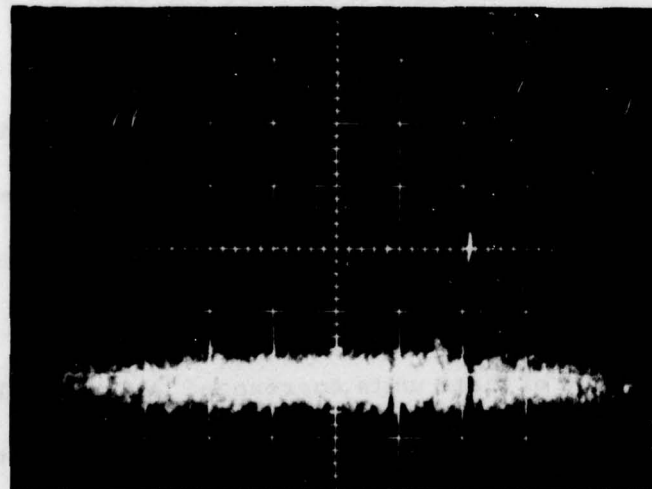
# TRACKING ACCURACY FOR 25 MV INPUT SIGNAL



HORIZONTAL POSITION (RELATIVE CLOCK COUNT)  
a. HORIZONTAL TRACKING ACCURACY



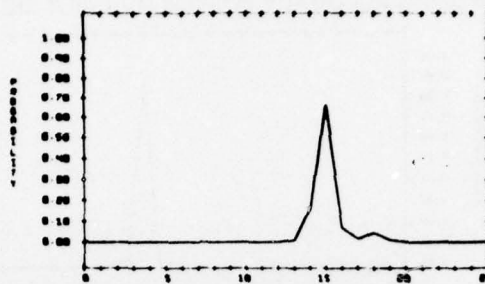
VERTICAL POSITION (RELATIVE LINE NUMBER)  
b. VERTICAL TRACKING ACCURACY



c. VIDEO CORRELATION SIGNAL

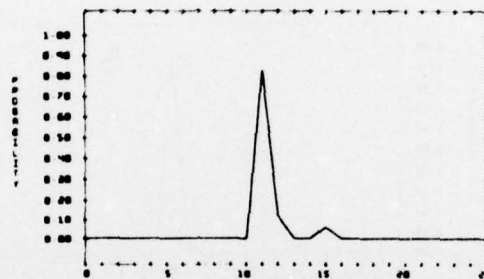
Figure 5.2-2 Tracking Accuracy and Video Signal for Input Correlation Peak of 25 mV

TRACKING ACCURACY FOR 100 MV INPUT SIGNAL



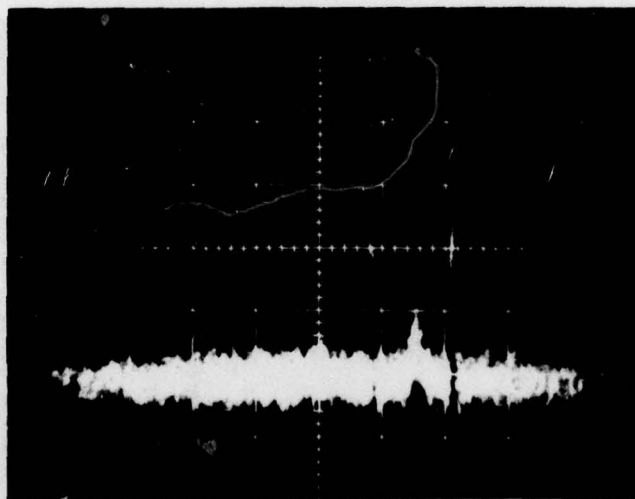
HORIZONTAL POSITION (RELATIVE CLOCK COUNT)

a. HORIZONTAL TRACKING ACCURACY



VERTICAL POSITION (RELATIVE LINE NUMBER)

b. VERTICAL TRACKING ACCURACY

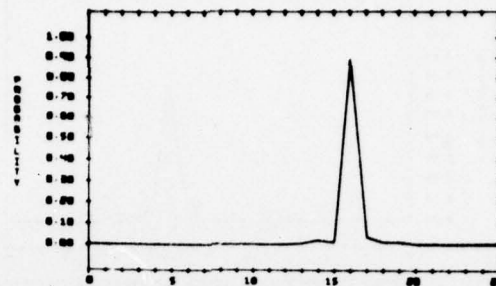


c. VIDEO CORRELATION SIGNAL

Figure 5.2-3 Tracking Accuracy and Video Signal for Input Correlation Peak of 100 mV

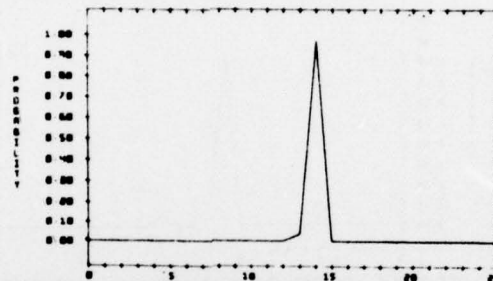


TRACKING ACCURACY FOR 200 MV INPUT SIGNAL



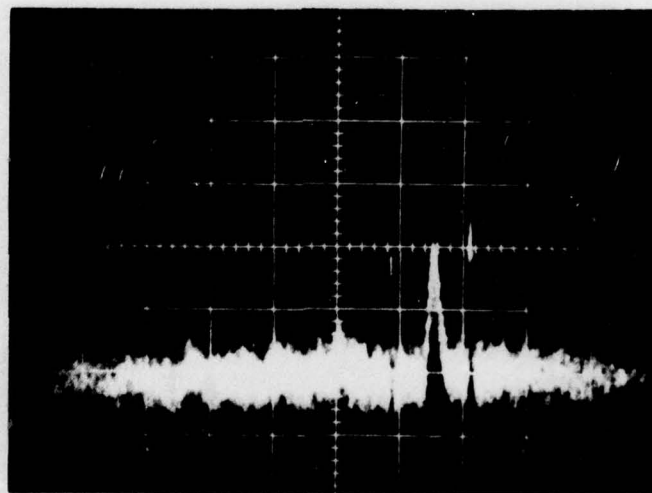
HORIZONTAL POSITION (RELATIVE CLOCK COUNT)

a. HORIZONTAL TRACKING ACCURACY



VERTICAL POSITION (RELATIVE LINE NUMBER)

b. VERTICAL TRACKING ACCURACY



c. VIDEO CORRELATION SIGNAL

Figure 5.2-4. Tracking Accuracy and Video Signal for Input Correlation Peak of 200 mV

The test of the interface electronics in a dynamic mode required the development of software capable of data collection at 30 samples per second. Software initially developed failed to reach this execution rate. However, refinements and modifications to the controlling software program were implemented which reduced execution time to acceptable levels. The primary change was the use of integer arithmetic rather than the normal floating point format. In this scheme, the correlation positional values, as well as the aperture location and the galvanometer addresses, are pure integers. Similarly, any computation or calculation involving these values must be performed in integer format, and care must be taken to ensure that proper results are obtained. In an operational sense, the integer formats are not significant drawbacks because any conversions to the floating point format can be accomplished off-line during a period when speed is not a paramount consideration. The final software program developed was capable of data collection at TV frame rates of 30 parallax samples per second.

The interface electronics were also tested in a dynamic mode. Although acceptable operation was achieved for very intense correlation signals, the overall performance was limited by several effects which were not present in the static tests. During the dynamic tests, all of the system functions were operational; the galvanometer scanning, aperture location and movement, and the peak detection features were used. The simultaneous

operation of these features generated additional noise in the correlation detection and location process. Computer clock noise was coupled into the video signal; this noise was reduced to acceptable levels by suitable low pass filtering. A ringing phenomena was observed in dynamic testing on the aperture boundaries. The ringing caused an uncertainty in the precise time and location of the aperture boundaries. However, the video gating circuitry, operating from a fixed clock signal, has a predetermined and periodic window. Because of the uncertainty in the aperture location, the gating circuit sometimes allowed undesired signals to reach the peak detector. The undesired signal was a portion of the aperture boundary. In regions where weak correlation signals were obtained, the aperture boundary (crosshairs) exceeded the intensity of the correlation signal and was erroneously identified as the actual correlation peak.

The software controlling program used a predictive algorithm to calculate the location of the aperture. The incorrect data points prevented proper action of the algorithm. The parallax data gathered with the system in a dynamic mode had significant variations because of the ringing problem.

Two approaches to correct this issue were identified. The first approach involved a refinement of the hardware design to take advantage of components which have recently become available. Integrated circuits to provide the gating function and the peak detection are now available



which satisfy operational requirements. Only a discrete electronic design was possible during the initial program phases. The substitution of the integrated circuits for the discrete electronics should significantly reduce the noise and ringing levels, and thus improve performance. The second approach was the implementation of a completely digital peak detection system. Component costs and cycle times for this approach have decreased significantly since original program funding. The digital peak detection approach is at this time a major candidate. In addition, the digital peak detection approach offers a greater potential for the feature extraction process; the approach is directly compatible with the digitizing process required to obtain, convert and manipulate selected features of an image. Further pursuit of these two approaches was outside the scope of current funding.

The technical effort for the program was terminated prior to the complete demonstration of system goals. A time delay was partially responsible for a considerable amount of labor expended to repair the government furnished galvanometer scanning system. The recurring failures of the galvanometer drivers, critical for system operation, prevented additional development of the interface electronics.

Despite the premature termination of the technical activity, all of the primary stereocompilation goals were partially demonstrated; these include:

- Solid state area sensor arrays were surveyed for possible use in correlation detection; a charge-injection device was selected and subsequently installed in the experimental system.
- Interface electronics necessary to perform automatic peak detection were designed, fabricated, and tested.
- The software control routines required to drive the parallax collection process were demonstrated at data sample rates of 30 frames per second.

#### Reference

- 1) "Parallax Measurement Using an Image Matched Filter Correlator", Final Technical Report for Contract F30602-73-C-0312, Prepared for Rome Air Development Center by the Electro-Optics Department of Harris Corporation.
- 2) "Image Matched Filter Correlator Experiments", Final Technical

Report for Contract F30602-75-C-0305, Prepared for Rome Air  
Development Center by the Electro-Optics Department of Harris  
Corporation.



## SECTION VI

### FEATURE EXTRACTION

The identification and subsequent location of patterns from aerial photographic imagery provides information of significant value to both government and civilian agencies. Government groups gather information relating to tactical weapon deployment and the development status of strategic areas. Similarly, civilian agencies routinely monitor earth resources and perform survey functions using aerial photography. Presently, the major portion of these efforts are performed manually by trained photo-interpreters. These interpreters, relying on past experience and developed skills, search individual frames of imagery to locate and catalog the patterns of interest. Although aided partially by computer data-logging techniques, this location and catalog process is tedious and slow. The increasing volume of imagery generated for analysis cannot be processed in a timely manner with manual techniques. To satisfy the critical demand for current and reliable information, an automated pattern recognition scheme must be developed.

Whether performed manually or automatically, the actual pattern recognition process involves three key steps. First, the features necessary to characterize and distinguish particular patterns must be determined. Second, these selected features must be extracted for the different areas

of the image. Third, the relevant data must be processed to classify or recognize the patterns of interest. These steps of feature selection, extraction, and classification must take into account variations in pattern appearance (e.g., shape, orientation, and scale) expected statistically both within a frame and between frames of aerial imagery; this capability is a major consideration for any pattern recognition process. The photo-interpreter relies on his experience and judgement in handling these variations; the automated process must possess a comparable capability.

The pattern recognition process can range from relatively simple tasks, such as separating urban and rural regions, to highly complex tasks, such as identifying aircraft types present at landing facilities. Similarly, the features associated with these tasks can vary over a wide spectrum. The selection of features to perform these tasks is often done in an intuitive or subjective fashion. A set of features which are felt to provide a separability between patterns or classes can be developed and subsequently tested. The effectiveness and completeness of the feature set are then evaluated in initial pattern recognition or class separation tests. Based on this evaluation, the original set of features can be modified to provide better performance. For example, a feature with little influence on the process

might be deleted, while another feature, not initially included in the feature set, might be added to provide a higher discrimination measure. In addition, various features can be altered to form linear and non-linear combinations which offer simplified processing or faster sorting time. This feature refinement process can be continued until satisfactory performance is achieved.

The selection of a set of features is a critical stage of the pattern recognition process. This feature set must be complete; that is, the features must adequately describe the patterns of interest and differentiate among them. The features must also be efficient to provide a maximum accuracy with minimum processing storage and time demands. In addition, the features must be relatively insensitive to the statistical variations in pattern appearance.

The major aim of the feature selection process is to choose the minimum number of features which preserve class separability. The effectiveness of the chosen feature set can be measured by the probability of error. This probability, affected by the scatter and variation encountered, is highly dependent on the particular recognition task at hand.

Pattern recognition from aerial photographs with a purely digital processing facility must rely primarily on a high resolution digital pixel representation of the image. From this representation other features can



be constructed. A low resolution pixel matrix can be developed for course recognition through averaging techniques. Various transforms, including the Fourier and Mellon transforms, can be calculated for different size regions of the image. The cross-correlation, yielding the parallax values for ground profiles, can be computed for stereo pairs of images. Low, high, and bandpass spatial filtering of the original pixel representation can be implemented through suitable software algorithms. However, all of these representations demand a significant amount of memory storage and require additional processing time.

An alternative or adjunct to scanning and digitally processing an image for feature extraction is the use of optical techniques directly on the image. A coherent optical processing system has considerable potential in the feature extraction area. An optical processing system, such as the IMF breadboard, provides direct access to the input imagery, the Fourier transform of that imagery, and a filtered version of the image. The simultaneous presence of these three elements in a single system is a unique situation having significant advantages for pattern recognition. In addition, these functions can be provided without a demand for digital memory storage or an increase in processing times; these are key considerations for feature extraction and subsequent pattern recognition.

A coherent optical processor can directly yield the digital pixel representation at various scales for aerial photographs. A simple modification to the scanning geometry of the IMF system would provide this capability. To accomplish this task, a set of lenses, mounted in a turret assembly whose position is computer controlled, is added to the scanning beam optics. Each lens is chosen to provide a different diameter scanning beam in the input plane of the processor. A single detector in the transform plane would collect all the light transmitted through the photograph; a single analog-to-digital converter sampling the detected energy would provide the pixel value for the given location and area of the scanning beam. By automatically selecting different lenses of the turret assembly, the computer could digitize the image at various resolutions. In addition, simple spatial filtering could be employed to obtain filtered versions of the imagery. For example, a transmissive or opaque disc located prior to the detector in the transform plane would allow a low or high passed filtered image to be digitized. Similarly, a transmissive annular filter in front of the detector would provide a spatially band-passed image to be digitized. The image could thus be digitized in a variety of formats with a coherent processing system. This sampling process is capable of high speeds; a digitizing rate of 50K pixels per second at 500 lpi resolution is feasible.

Power spectral analysis can also be directly implemented with the IMF

system. The transform plane of the IMF system contains a light intensity distribution which is the spatial frequency power spectra of the image in the input plane. The measurement of the intensity distribution can be simply accomplished by locating a two dimensional solid-state area array in the transform plane; analog-to-digital conversion of the resulting signal provides a digital representation of the power spectra at video bandwidths. The power spectra can thus be measured directly at high rates instead of calculated or computed from digital pixel representations. In addition, since the scanning system can access different locations of the input image and provide a range of scanning spot diameters, the power spectra can be determined directly for localized regions of the image. Thus, changes in the spectra for various local regions could be detected and utilized for feature extraction.

A conventional two dimensional array, such as a CID used in conjunction with an a/d converter and a digital computer can be used to synthesize unique, specially shaped apertures in the transform plane. For instance, a series of concentric rings and radial wedges (similar to those of the Recognition System ROSA detector) can be simulated. Although this pattern is simplistic, successful photograph sorting has been demonstrated in relatively simple applications. The value of the ring and wedge detector pattern

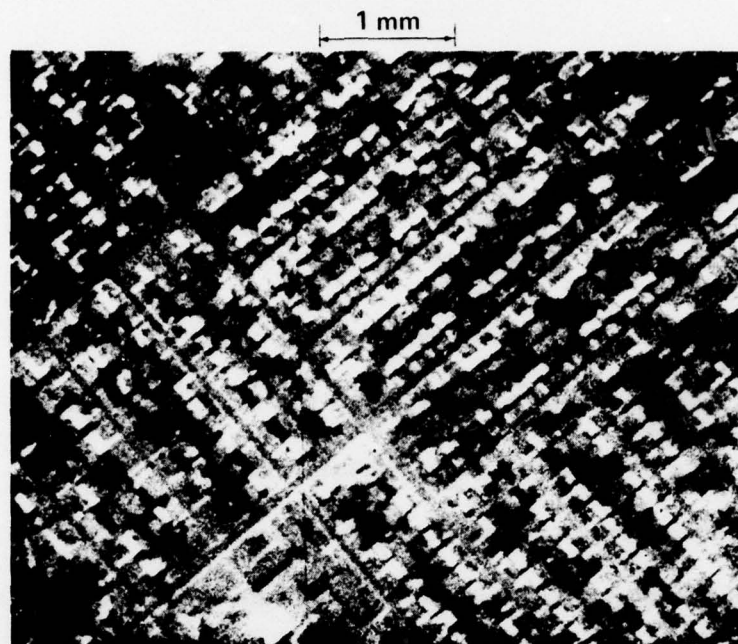


for feature extraction requires further investigation.

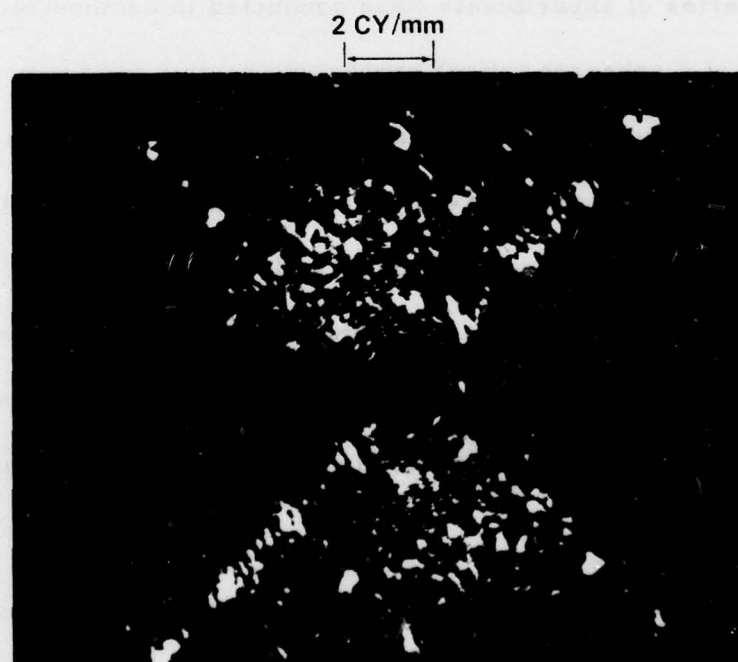
The IMF system can provide another feature measure for pattern recognition; parallax can be determined for local areas of the image. The parallax value can discriminate certain classes of terrain. For example, the frequent and large parallax changes characterizes some terrain regions (such as mountains and urban areas), but not others (such as agricultural regions and bodies of water). Parallax measurements have potential as an effective feature for pattern recognition.

A series of experiments were conducted to demonstrate the preliminary value of a coherent optical processing system for feature extraction and pattern recognition. Conventional contact copying techniques were used to generate sample imagery on high resolution plates from typical aerial photographs. The processed images were placed in the input plane of the IMF system, and their power spectra were observed. For the experiments, a scanning beam diameter of 5 mm was used for illumination and a DC block was located in the transform plane to eliminate the low frequency component.

Sections of different terrain regions and the corresponding power spectra are shown in Figures 6-1 through 6-3. Three different terrain types were selected which include an urban area, an airway landing faci-

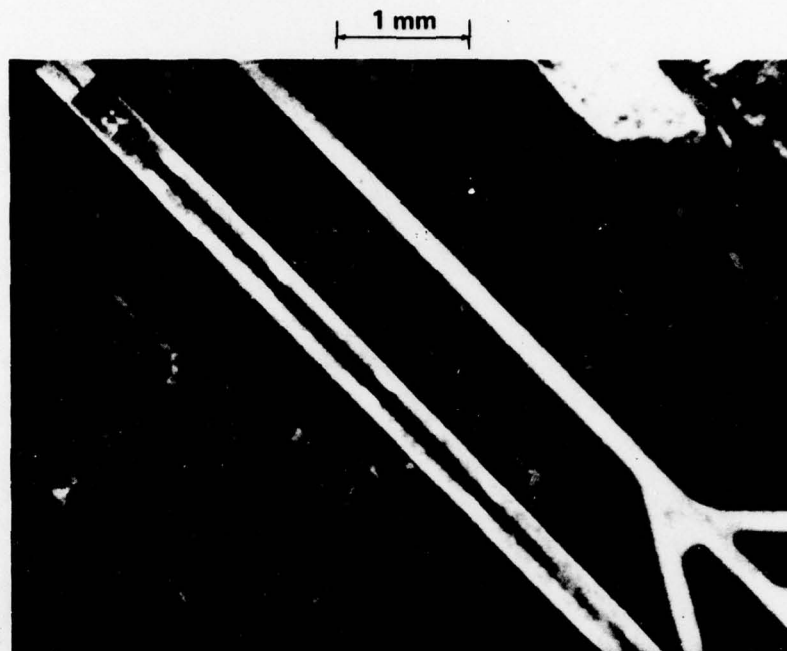


a. SECTION OF ORIGINAL AERIAL PHOTOGRAPH



b. CORRESPONDING POWER SPECTRUM

Figure 6-1 Image and Power Spectrum of Typical Urban Area



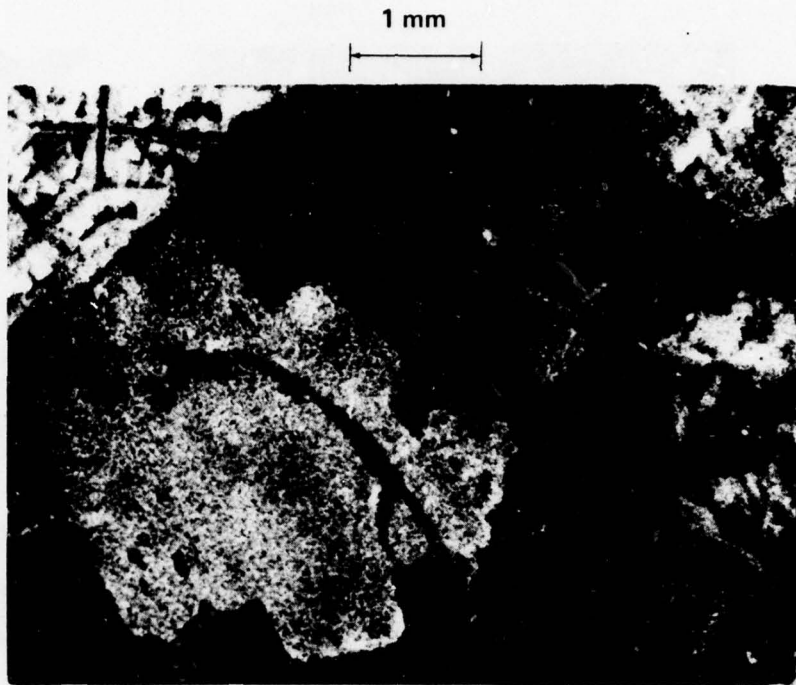
a. SECTION OF ORIGINAL AERIAL PHOTOGRAPH



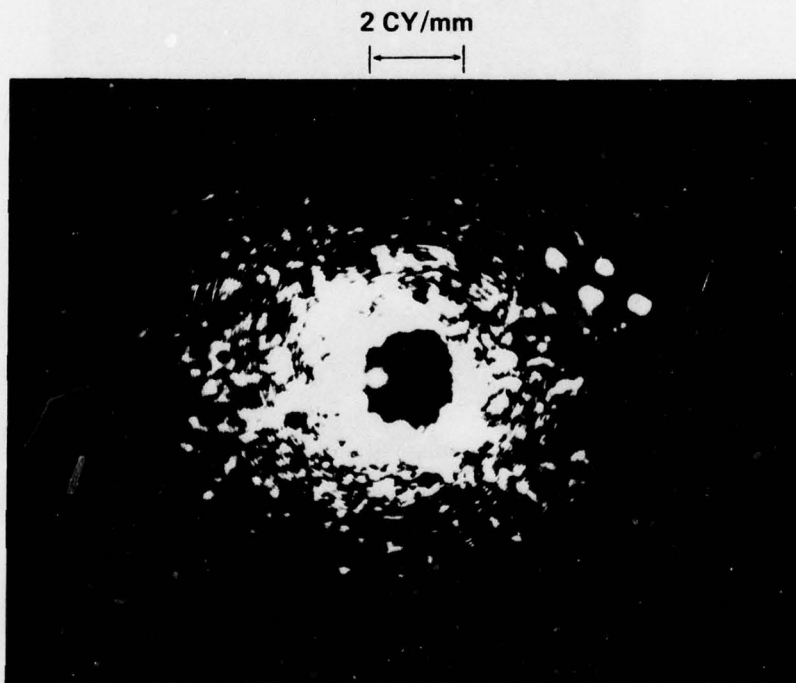
b. CORRESPONDING POWER SPECTRUM

Figure 6-2 Image and Power Spectra of Airway Landing Facility





a. SECTION OF ORIGINAL AERIAL PHOTOGRAPH



b. CORRESPONDING POWER SPECTRUM

Figure 6-3 Image and Power Spectra of Rural Terrain

lity, and a rural region. The urban region, shown in Figure 6-1 (a), contains a housing development with well-defined features; the houses and streets form a two dimensional pattern with a reasonably periodic structure. This regularity is evidenced in the power spectra shown in Figure 6-1 (b) by the cross-like transform pattern is caused by the regular edges and even features of the housing development. A similar result occurs for the airway landing facility shown in Figure 6-2(a). The sharp edges and constant orientation of the runway generate a Fourier transform of Figure 6-2 (b) having significant energy in only one direction.

Fine scale, continued features of an image are represented in the transform plane by an intensity pattern perpendicular to the feature direction. Typically, man-made objects are characterized by fine-scale, continued features which have regular structure. Examples include roads, housing developments, and urban centers. The detection of preferred or high intensity axes in the transform plane indicate structure associated with regular characteristics and yield information on their orientation.

For comparison, a rural region and its power spectrum are shown in Figure 6-3. The rural region shown in Figure 6-3 (a) is devoid of man-made structures and exhibits no regular or periodic structure. The associated power spectra of figure 6-3 (b) similarly has no preferred dir-

ection or characteristics. The intensity of the transform decreases in a uniform radial fashion.

Additional investigation of the feature extraction and pattern recognition capabilities of coherent optical processing is warranted. The three figures demonstrate the effectiveness of a simple feature, the directional dependence of the Fourier transform, in separating or sorting man-made and rural terrain regions. With immediate access to the Fourier transform, a coherent processing system could perform the separation simply, directly and accurately. The results of the separation operation could be used to pre-screen imagery for subsequent manual or digital classification or to provide initial estimates of terrain boundaries for additional optical recognition.

While coherent optical processing for feature extraction is promising, there is no guarantee that this technique will be highly successful and, in any case, a fairly significant technical effort will be required to develop and prove an operational system. On the other hand, the same comments can be applied to digital processing of scanned imagery. There certainly is hope that truly competent systems for feature extraction and classification can be developed; coherent optical processing could be a significant portion of this system. However, the problem is one of great difficulty and



requires the establishment of a long range, well directed program.

## APPENDIX A

### CIRCUIT SCHEMATICS FOR IMF INTERFACE ELECTRONICS

This appendix details the components and connections utilized in the IMF interface electronics. The appendix includes the circuit diagrams for the computer interface, the aperture location module, and the track/hold circuits. In addition, the analog electronic circuit which performs the peak detection is included. A full description of system operation is presented in Section 5.1.2.

3



DATE	NEXT ASSY	USED ON
APPLICATION		

UNLESS OTHERWISE SPECIFIED  
DIMENSIONS ARE IN INCHES  
AND INCLUDE APPLIED FINISH  
TOLERANCES  
2 PLACE DIM 3 PLACE DIM ANG



3

2

1



6

23

1

1

3

2

1

AD-A065 044

HARRIS CORP MELBOURNE FL ELECTRO-OPTICS DEPT  
AUTOMATIC CORRELATION MEASUREMENT EXPERIMENTS.(U)  
DEC 78 F B ROTZ, M W SHARECK

F/G 5/8

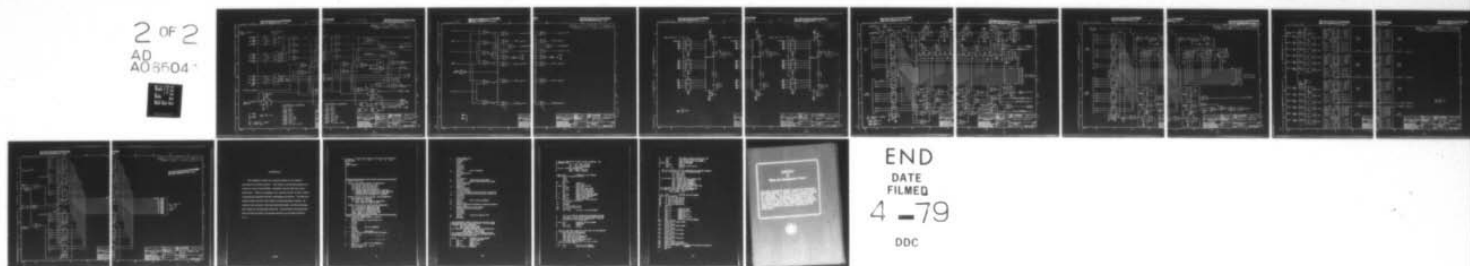
UNCLASSIFIED

RADC-TR-78-250

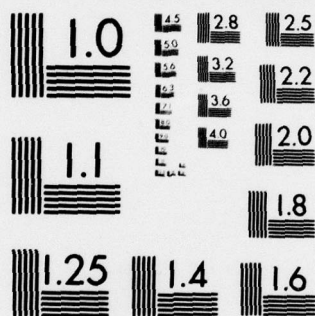
F30602-76-C-0381

NL

2 OF 2  
AD  
A065044



END  
DATE  
FILMED  
4 -79  
DDC



MICROCOPY RESOLUTION TEST CHART  
NATIONAL BUREAU OF STANDARDS-1963-A



THIS PAGE IS BEST QUALITY PRACTICABLE  
FROM COPY FURNISHED TO DDC

U S BLUE PRINT PAPER CO CLEARPRINT 1000M

FROM 07 NIBUS  
LINES

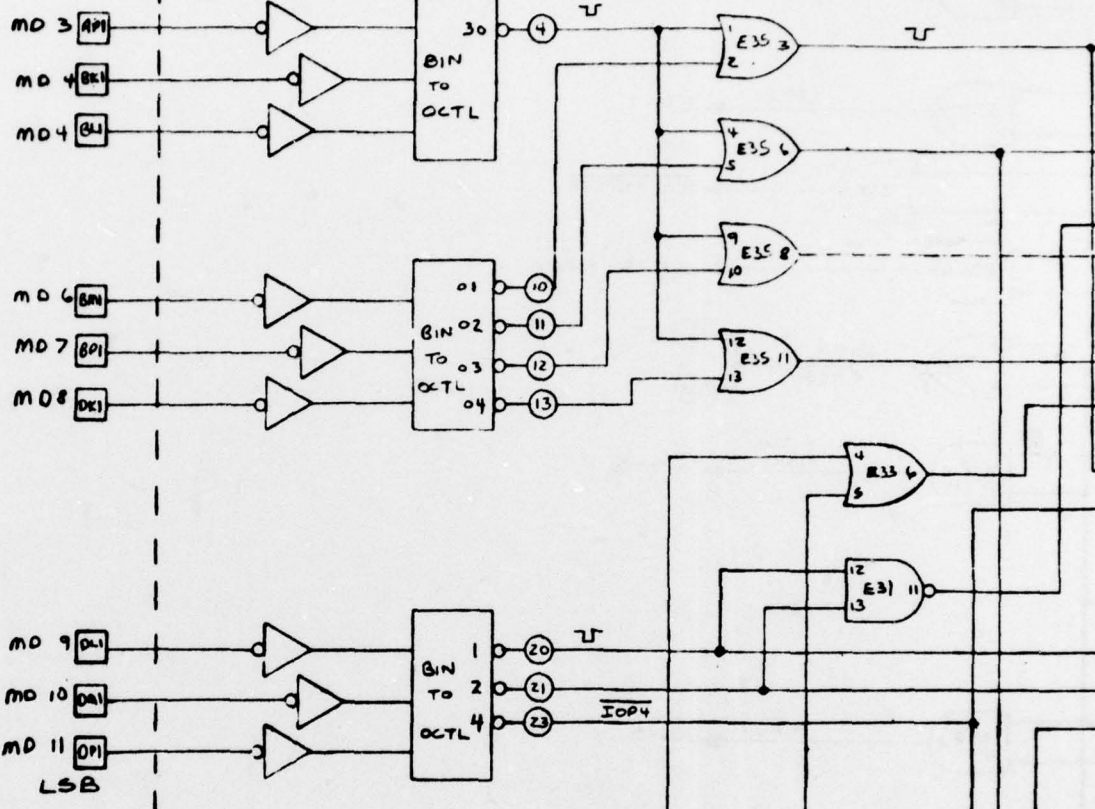
DEVICE ADDRESS  
DECODE

D

C

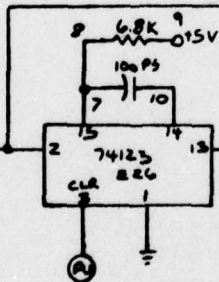
B

A



2<sup>ND</sup> FIELD EX-7

END OF EX-10  
APERTURE



E24 - COMPONENT CARRIER  
E36 - CABLE CONN.

# INTERFACE COMMANDS

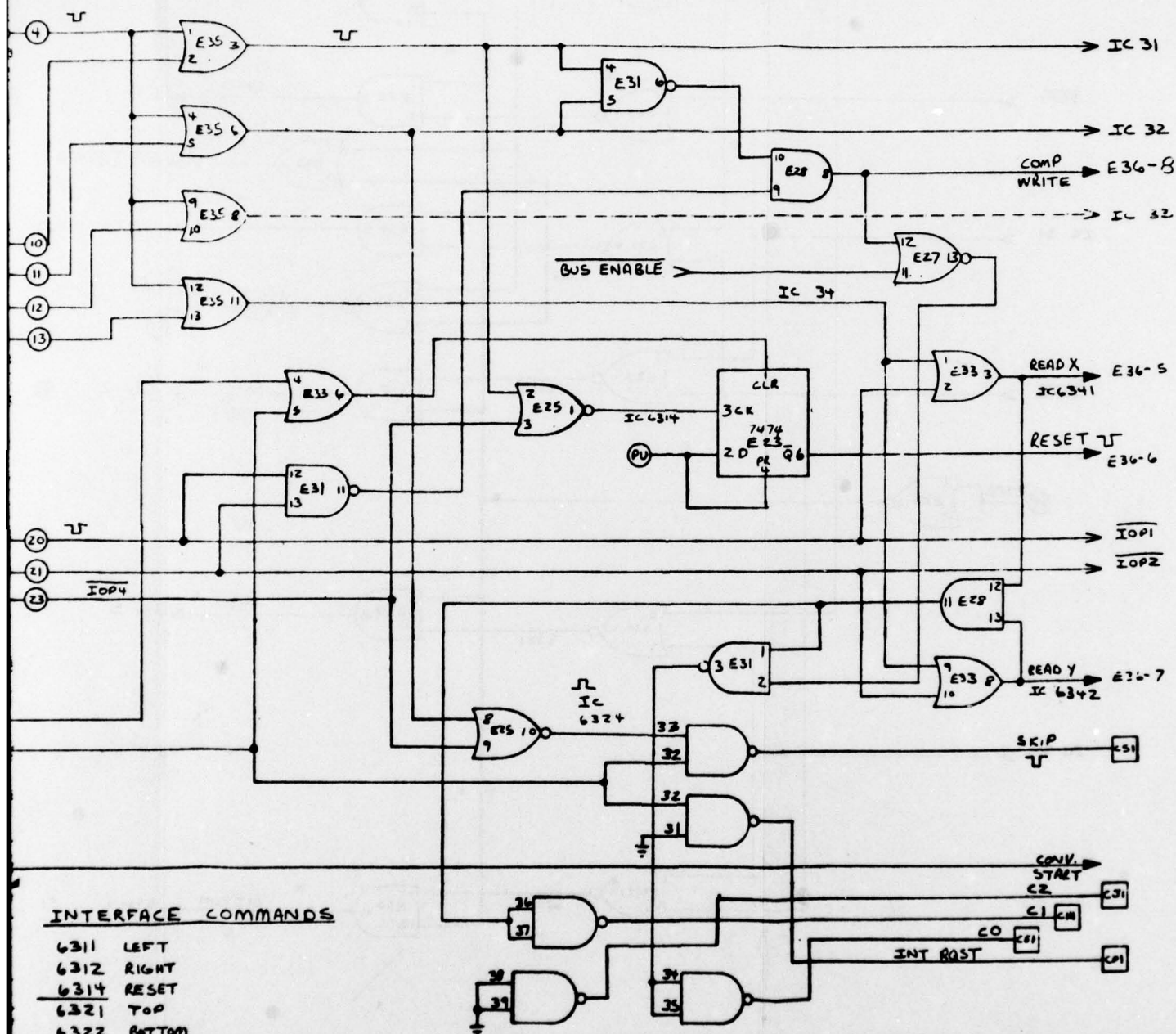
- 6311 LEFT
- 6312 RIGHT
- 6314 RESET
- 6321 TOP
- 6322 BOTTOM
- 6324 FLAG
- 6331 D/A X POS
- 6332 D/A Y POS
- 6341 PEAK X
- 6342 PEAK Y
- 635X A/D DEVICE SELECT

Y PRACTICABLE  
DC 3

THIS PAGE IS BEST QUALITY PRACTICABLE  
FROM COPY FURNISHED TO DDC

REVISIONS				DATE	APP	BY
ZONE	LTR	DESCRIPTION	DATE	APP	BY	
		CHG BY	CHG BY	FOUND		

RESS



# INTERFACE COMMANDS

6311 LEFT  
6312 RIGHT  
6314 RESET  
6321 TOP  
6322 BOTTOM  
6324 FLAG  
6331 D/A X POS  
6332 D/A Y POS  
6341 PEAK X  
6342 PEAK Y  
635X A/D DEVICE SELECT

HARRIS Melbourne F.O. 24 32101	
TITLE COMPUTER INTERFACE FOR POP 8/A	CODE IDENT NO. 91417
APPLICATION ABBREVIATIONS PER MIL-STD-12 LOGIC SYMBOLS PER MIL-STD-883C ELECTRICAL AND ELECTRONIC DIAGRAM PER USAS ELECTRICAL AND ELECTRONIC DIAGRAM PER USAS Y22.2 ELECTRICAL AND ELECTRONIC REFERENCE	SHEET 1 OF 3

3

2

1

1

89

THIS PAGE IS BEST QUALITY PRACTICABLE  
 FROM COPY FURNISHED TO DDG

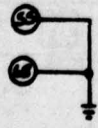
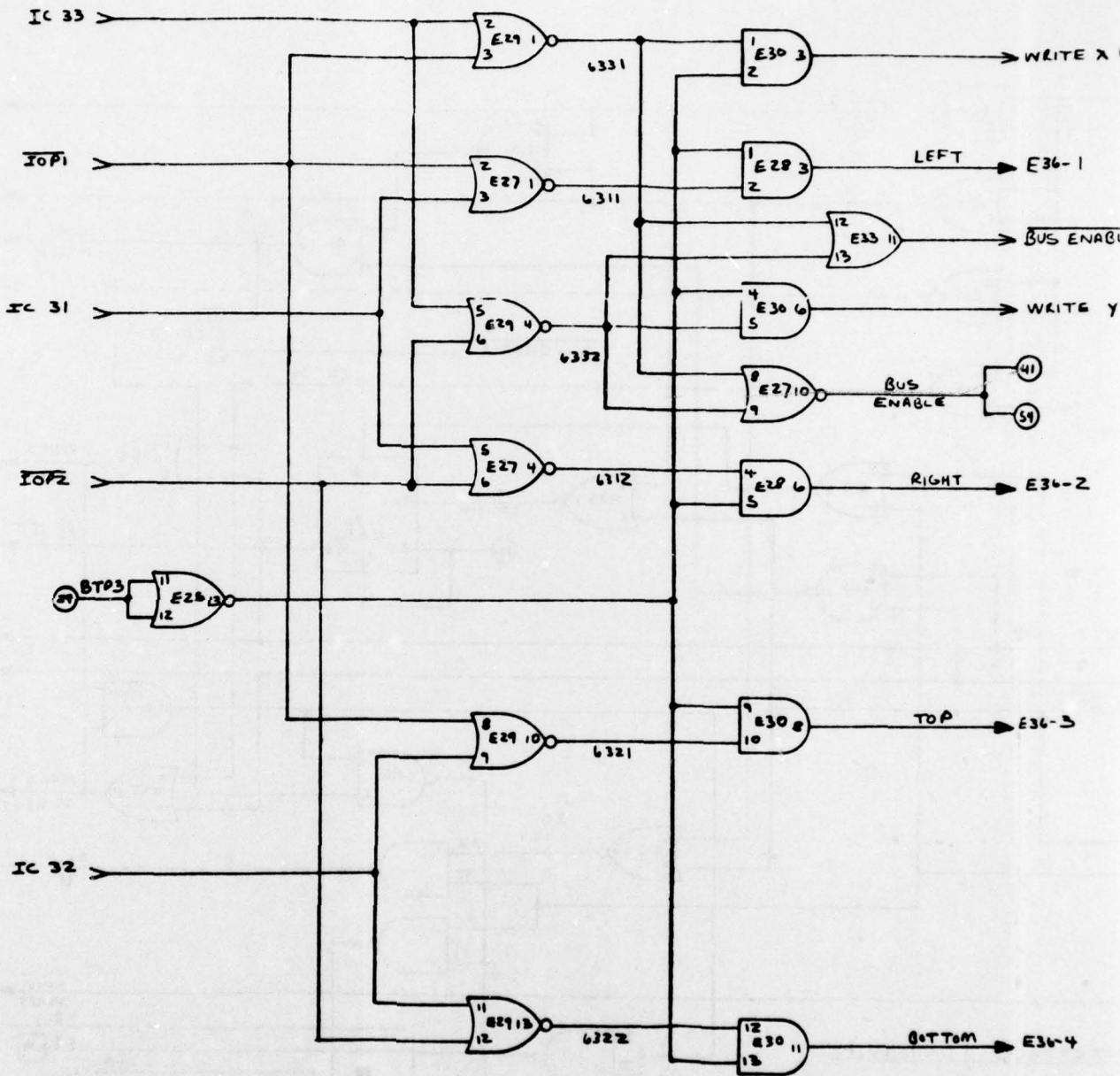
U S BLUE PRINT PAPER CO. CLEARPENT 100-

D

C

B

A

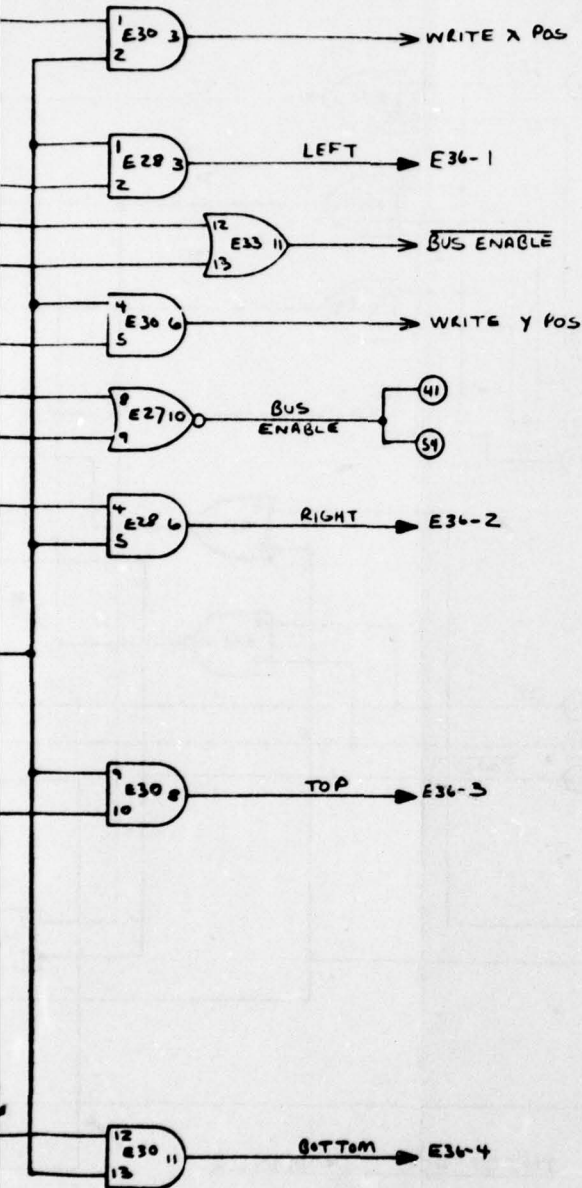


DATE	NEXT ASSY
APPLICAT	
ABBREVIATIONS PER MIL STD	
LOGIC SYMBOLS PER MIL STD	
ELECTRICAL AND ELECTRONIC	
ELECTRONIC DIAGRAM PER US	
ELECTRICAL AND ELECTRONIC	



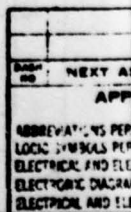
THIS PAGE IS BEST QUALITY PRACTICABLE  
FROM COPY FURNISHED TO DDC

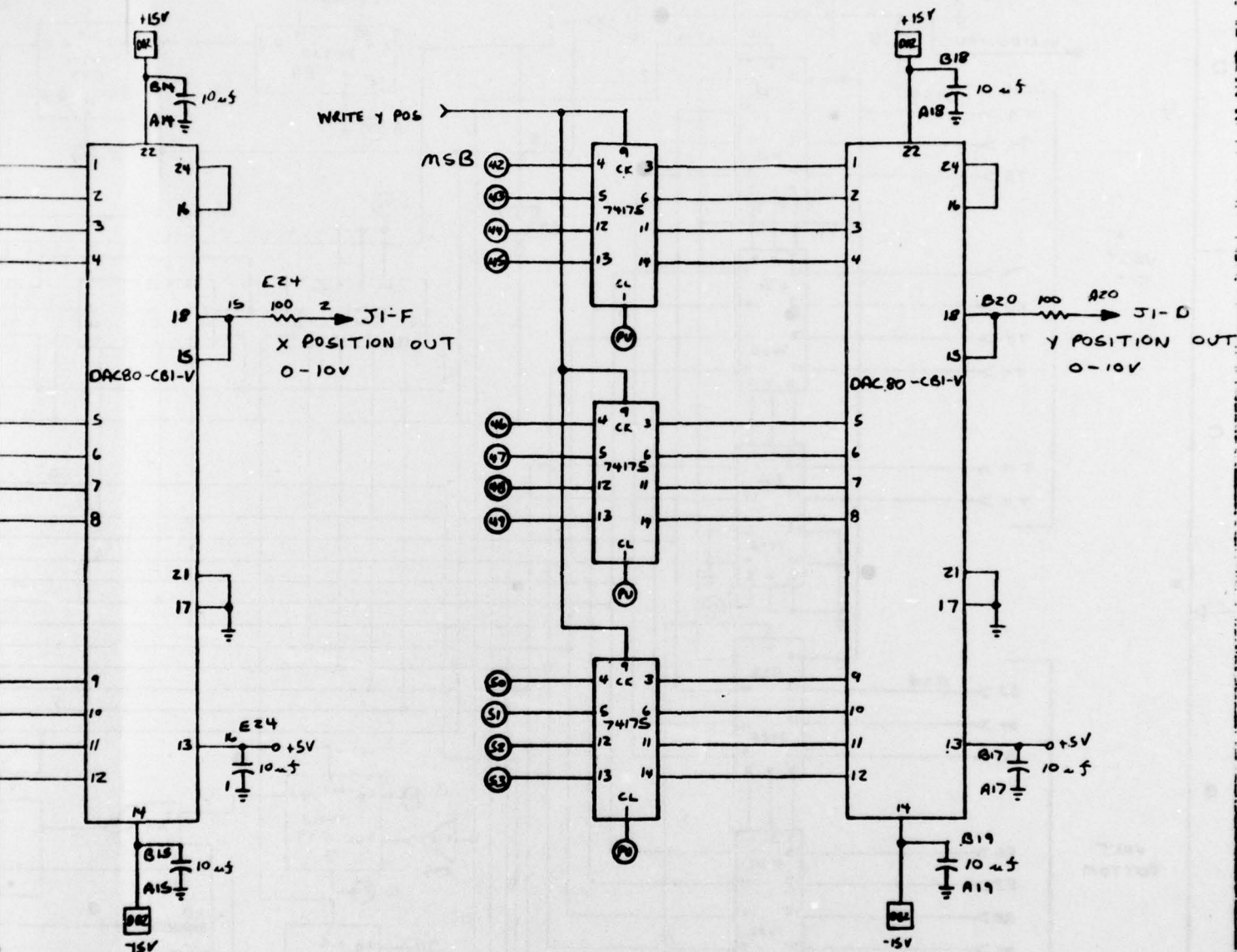
REVISIONS					DATE	APPROVED
ZONE	LTR	DESCRIPTION	CHG BY	SCD BY		



HARRIS Melbourne, Florida 32901		TITLE COMPUTER INTERFACE FOR POP-8A	
APPLICATION ABBREVIATIONS PER MIL-STD-12 LOGIC SYMBOLS PER MIL-STD-400 ELECTRICAL AND ELECTRONIC DIAGRAM PER USAS ELECTRONIC DIAGRAM PER USAS Y12.2 ELECTRICAL AND ELECTRONIC REFERENCE		SIZE 91417	
NEXT ASSY USER ON		SCALE SHEET 2 OF 3	

M &amp; S BLUE PRINT PAPER CO. CLEARPRINT 1000M





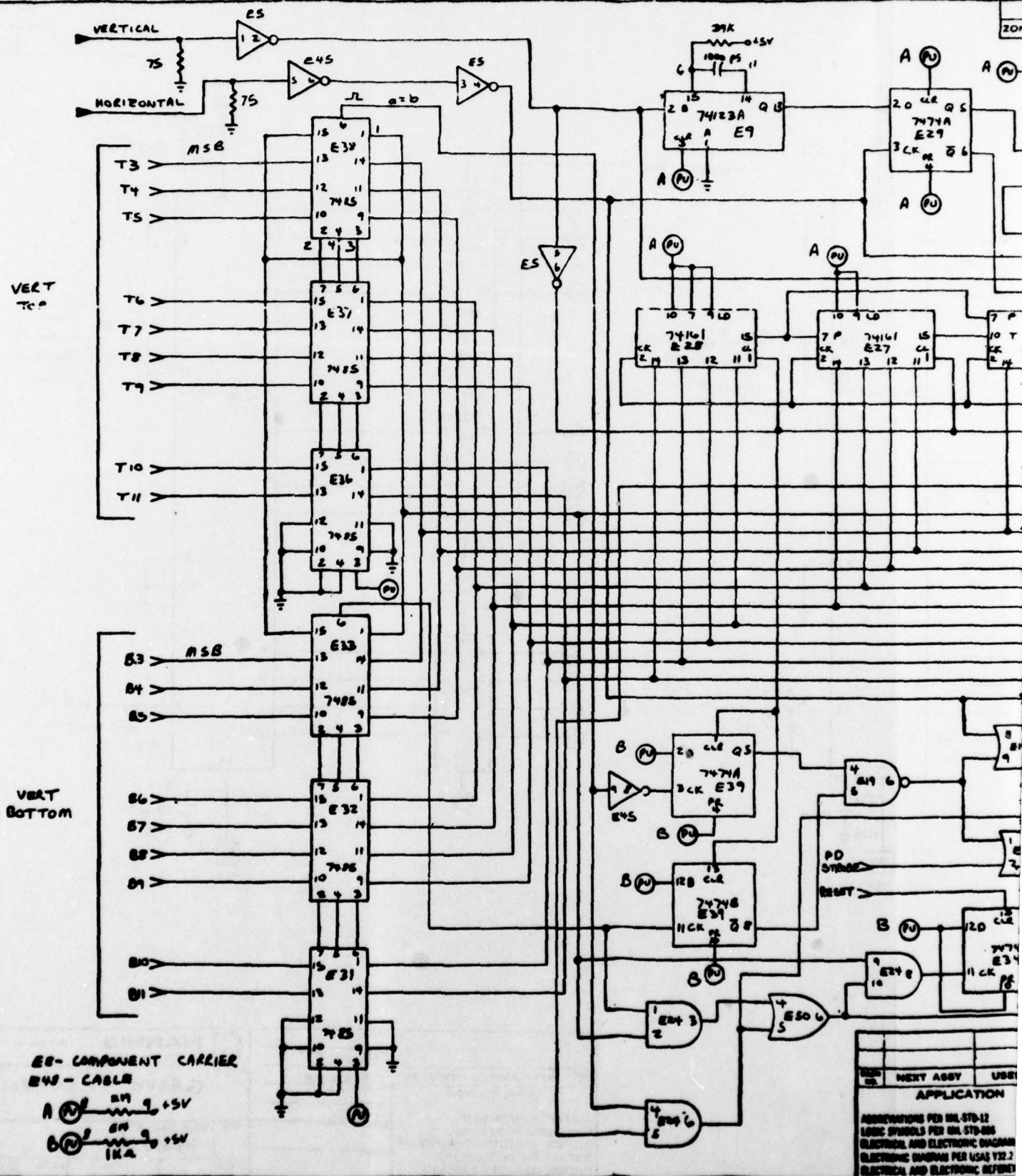
CONTROLLER NO.		HARRIS	
DATE		Model No. 74175	
NEXT ASSY		USED ON	
APPLICATION		TITLE	
ABBREVIATIONS PER MIL-STD-12		SIZE	
LOCAL SYMBOLS PER MIL-STD-883		CODE IDENT NO.	
ELECTRONIC AND ELECTRICAL DIAGRAM PER USAS		91417	
ELECTRONIC DIAGRAM PER USAS Y32.2		SCALE	
ELECTRONIC AND ELECTRONIC REFERENCE		SHEET 3 of 3	



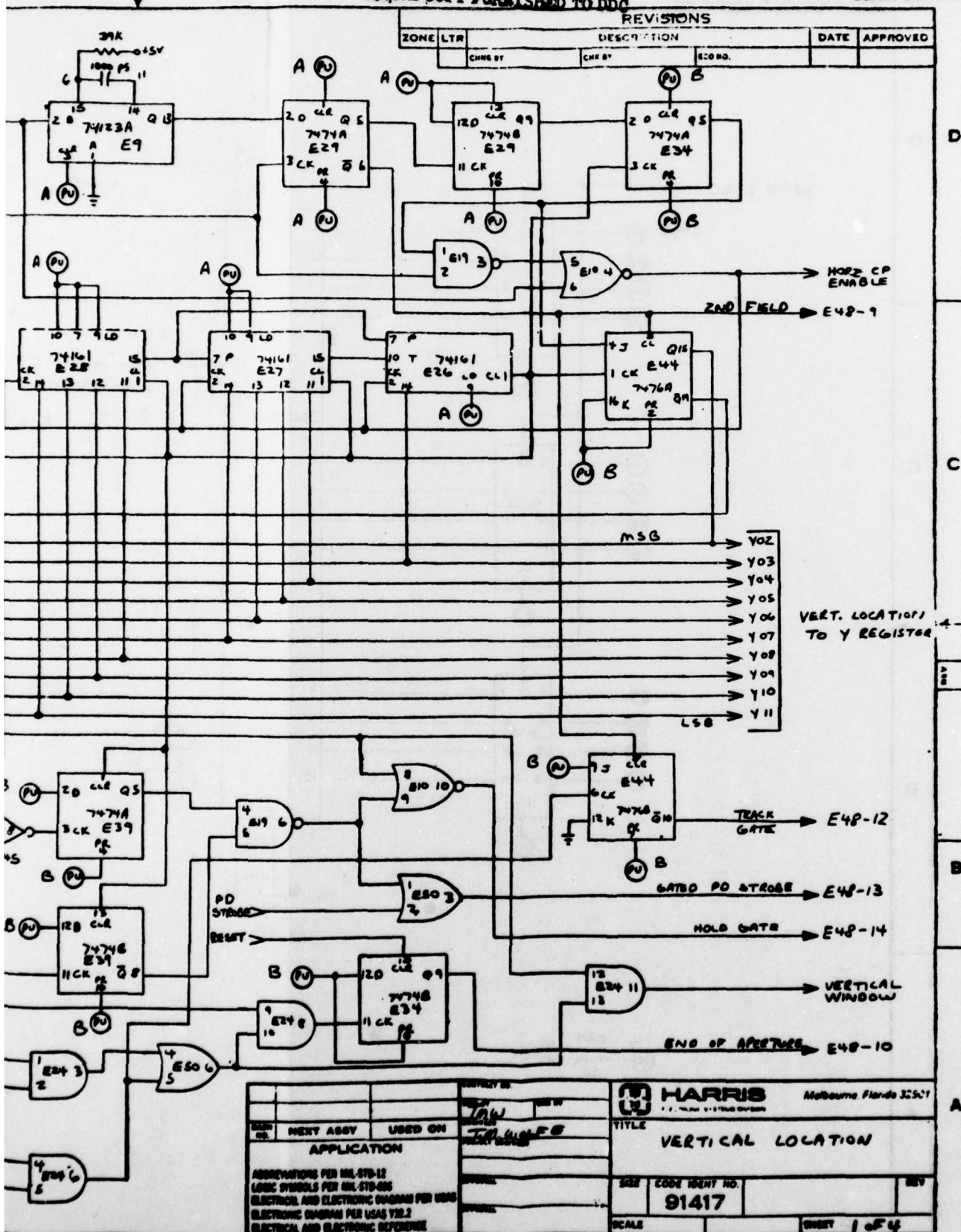
THIS PAGE IS BEST QUALITY PRACTICALLY  
FROM COPY FURNISHED TO DDG

THIS  
FROM

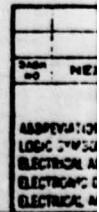
U S BLUE PRINT PAPER CO CLEARPOINT 1000H



THIS PAGE IS BEST QUALITY PRACTICABLE  
FROM COPY FURNISHED TO DDC



CHAPIN 7-1700 100

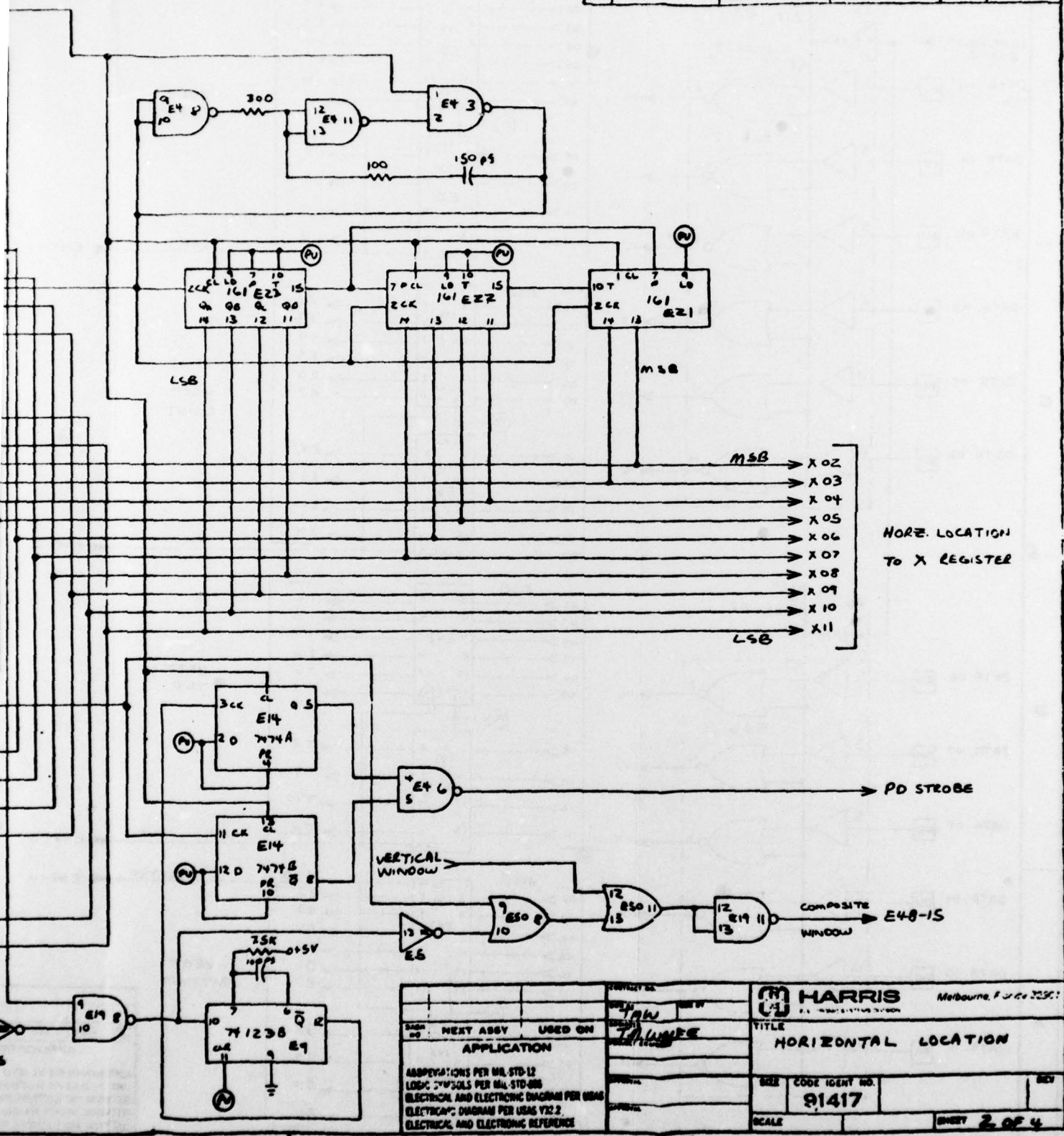




QUALITY PRACTICABLE  
ED TO DDG

THIS PAGE IS BEST QUALITY PRACTICABLE  
FROM COPY FURNISHED TO DDG

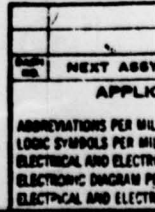
REVISIONS		DATE	APPROVED
ZONE	LYR		
CHRG BY	CHRG BY	ECNO.	



HARRIS Melbourne, Florida 33501	
TITLE HORIZONTAL LOCATION	
CODE IDENT NO. 91417	
SCALE SHEET 2 OF 4	
APPROVATIONS PER MIL-STD-12 LOGIC SYMBOLS PER MIL-STD-883 ELECTRICAL AND ELECTRONIC DIAGRAM PER IEEE ELECTRICAL AND ELECTRONIC REFERENCE	
NEXT ASSY USED ON APPLICATION	
DESIGN BY DATE	
CHECKED DATE	

2

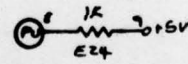
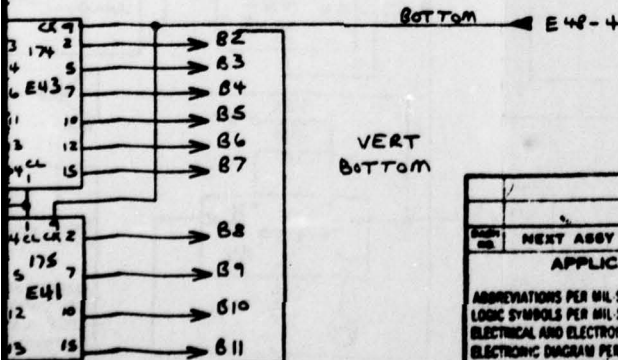
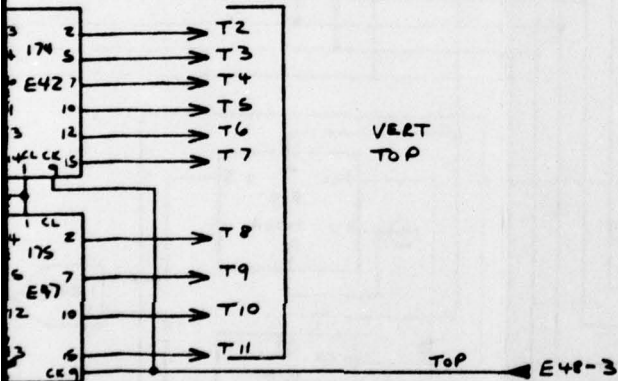
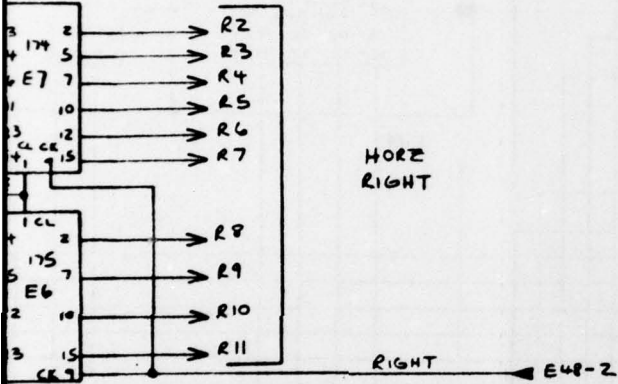
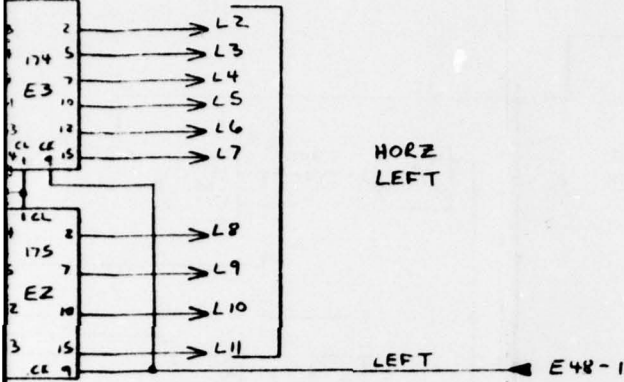
U S BLUE PP 4" PAPER CO C, FANPRINT 1000H



QUALITY PRACTICABLE  
ED TO DDG

THIS PAGE IS BEST QUALITY PRACTICABLE  
FROM COPY FURNISHED TO DDG

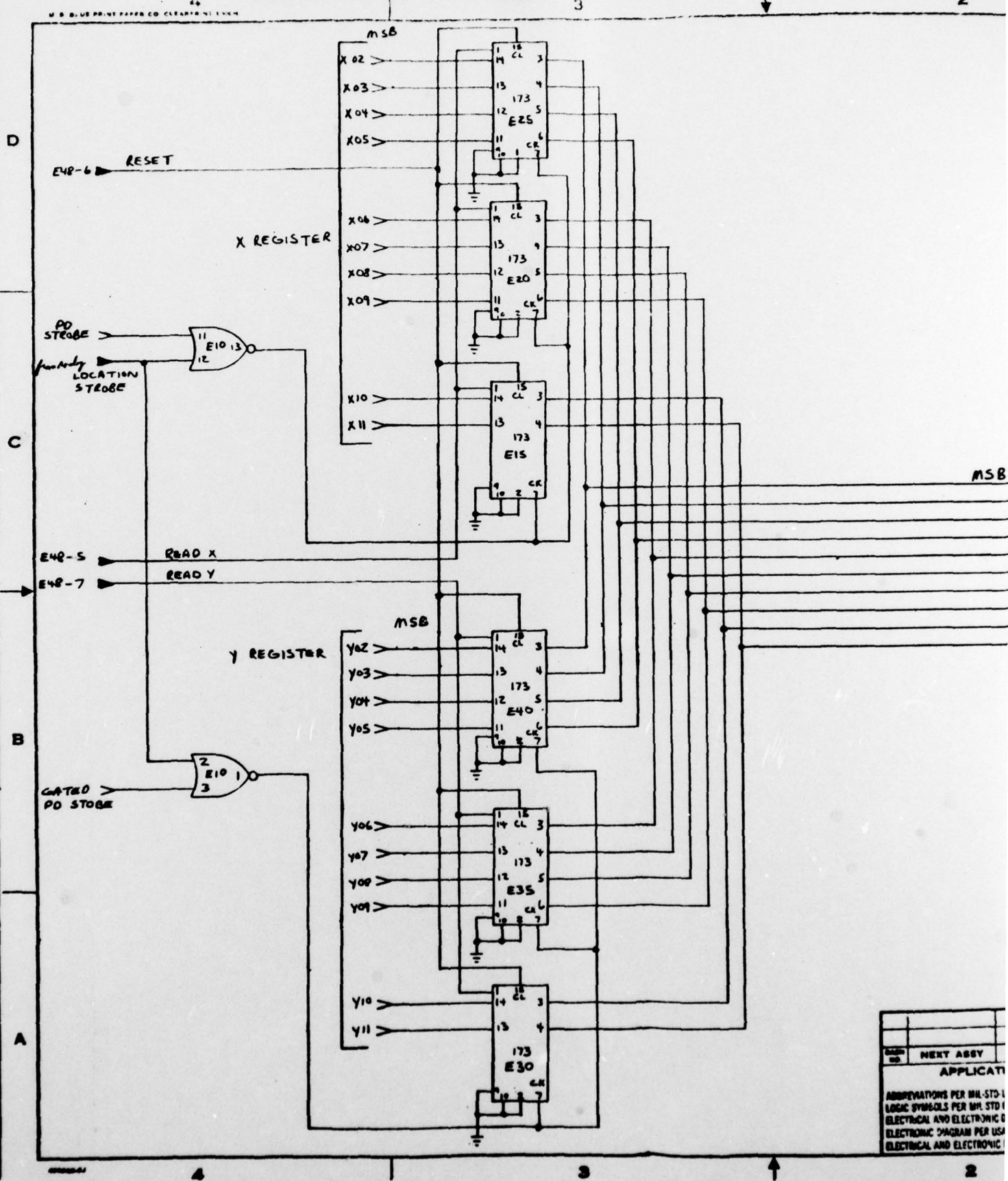
REVISIONS				
ZONE	LTR	DESCRIPTION		DATE
		CHNG BY	CHK BY	ACC NO.



NEXT ASSY USED ON		HARRIS Melbourne, Florida 32901	
APPLICATION ABBREVIATIONS PER MIL STD-12 LOGIC SYMBOLS PER MIL STD-808 ELECTRICAL AND ELECTRONIC DIAGRAM PER USAS ELECTRONIC DIAGRAM PER USAS Y32.2 ELECTRICAL AND ELECTRONIC REFERENCE		TITLE COMPUTER INTERFACE FOR POP 8/A	
SIZE CODE IDENT NO. 91417		REV	
SCALE		SHEET 3 OF 4	



THIS PAGE IS BEST QUALITY PRACTICABLE  
FROM COPY FURNISHED TO DDG



CTICABLE

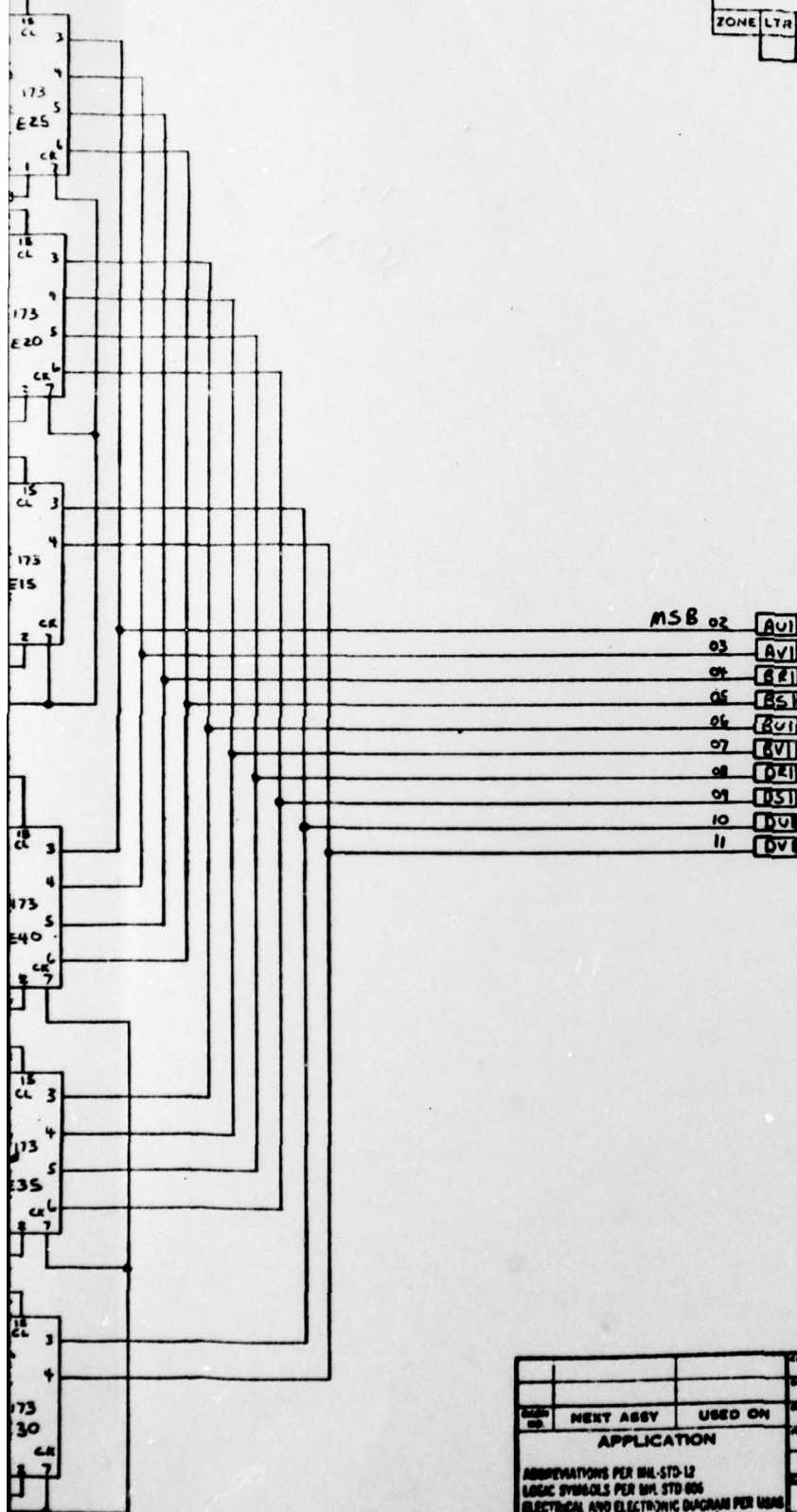
3

2

1

REVISIONS				
ZONE	LTR	DESCRIPTION	DATE	APPROVED
	CHG BY	CHK BY	ECO NO.	

THIS PAGE IS BEST QUALITY PRACTICABLE  
FROM COPY FURNISHED TO DDG



TO COMPUTER  
DATA BUS  
INVERTED  
DATA

CONTRACT NO.		HARRIS Melbourne Florida 32901	
DATE OF ORDER	DATE OF DELIVERY	TITLE COMPUTER INTERFACE FOR PDP-8A	
NEXT ASSY	USED ON	SIZE	CODE IDENT NO. 91417
APPLICATION ABBREVIATIONS PER MIL-STD-12 LOGIC SYMBOLS PER MIL-STD-883 ELECTRICAL AND ELECTRONIC DIAGRAM PER USAS Y32.2 ELECTRONIC DIAGRAM PER USAS Y32.2 ELECTRICAL AND ELECTRONIC REFERENCE		SCALE	SHEET 4 OF 4

3

2

1

1

95/96

2

## APPENDIX B

This appendix contains the program listings for the software developed for the IMF interface. The software controlling programs are written in Fortran-II and SABR, compatible with the DEC OS-8 operating system. These two languages were selected because of their relative programming simplicity and their interfacing convenience. The interface options support the drive and control of the galvanometer scanner, the selection and operation of the peak detection module, and the processing and storage for parallax data collection. The flowchart for system operation and the description of program functions are included in Section 5.1.3.





```

3      FORMAT(4MENUF,F3.1)
      IF (ENUF)4,1,1
4      CONTINUE
      IX=IX1
      IY=IY1
      IX1=IX-15
      IX2=IX+15
      IY1=IY-15
      IY2=IY+15
8      JMS AP          /SET UP APERTURE
5      CONTINUE
      DO 20 M=300,1500,4
      N=M/6-49
      IGX=M
      IGY=M
      DO 10 NF=1,N1
8      JMS GALVO      /MOVE GALVO TO SCAN POINT
8      JMS PEAK      /SAMPLE LOCATION AND PEAK HEIGHT
      JXA(N)=JXA(N)+JXL
      JYA(N)=JYA(N)+JYL
      JAMP(N)=JAL
10     CONTINUE
      JXA(N)=JXA(N)/N1
      JYA(N)=JYA(N)/N1
      IF (N-5) 15,15,12
12     IX=(JXA(N-4)+JXA(N-3)+JXA(N-2)+JXA(N-1)+JXA(N))/5
      IY=(JYA(N-4)+JYA(N-3)+JYA(N-2)+JYA(N-1)+JYA(N))/5
15     IX1=IX-15
      IX2=IX+15
      IY1=IY-15
      IY2=IY+15
8      JMS AP          /SET UP INITIAL APERTURE
20     CONTINUE
      WRITE (1,30)
30     FORMAT(6X,5HINDEX,6X,5HXPOSN,6X,5HYPOSN,6X,5HAMPTD)
      DO 50 N=1,201
      WRITE(1,45)N,JXA(N),JYA(N),JAMP(N)
45     FORMAT(6X,15,6X,15,6X,15,6X,15)
      IX1=JXA(N)
      IX2=JXA(N)
      IY1=JYA(N)
      IY2=JYA(N)
8      JMS AP          /TRACE THE PARALLAX PATH
50     CONTINUE
      GO TO 800

```

C THIS SUBROUTINE IS USED TO CONTROL THE OUTPUTS TO THE  
 C TWO GALVO DRIVERS IN THE ACME SYSTEM. THE TWO INTEGER  
 C ARGUMENTS AND THEIR RANGES ARE:  
 C     0   <IGX(X GALVO DRIVER)<2046  
 C     0   <IGY(Y GALVO DRIVER)<2046  
 C THE IMPORTANT INTERFACE COMMANDS FOR THE ROUTINE ARE:  
 C     6331--OUTPUT X GALVO VALUE  
 C     6332--OUTPUT Y GALVO VALUE  
 C THE VALUES,WHICH ARE PRESENT IN THE ACCUMULATOR,ARE  
 C D/A CONVERTED AND ROUTED TO THE GALVO DRIVERS WHEN THE  
 C OUTPUT COMMANDS ARE ENCOUNTERED.

```

S GALVO.      0000      /REMEMBER CALLING ADDRESS
S      CLA          /PREPARE FOR SHOVE
S      TAD \IGX      /LOAD X VALUE
S      6331         /SHOVE IT
S      TAD \IGY      /LOAD Y VALUE
S      6332         /SHOVE IT
S      JMP I GALVO   /GO BACK-

```

```

C THIS IS A SUBROUTINE TO READ THE ACME INTERFACE.  THE
C ARGUMENTS ARE:
C          JXL -- THE X PEAK LOCATION
C          JYL -- THE Y PEAK LOCATION
C          JAL -- THE PEAK AMPLITUDE
C THE KEY INTERFACE COMMANDS ARE:
C          6341 -- READ X LOCATION
C          6342 -- READ Y LOCATION

```

```

S PEAK, 0000          /REMEMBER CALLING ADDRESS
C MUST READ THE INTERFACE LOCATION
          JXL=0
          JYL=0
          JAL=0
310  CONTINUE
S      CLA            /CLEAR AC
S      6314           /RESET FLAG
S SYNC, 6324          /SKIP WHEN FLAG SET
S      JMP SYNC       /WAIT LOOP
S      JMS ADC        /READ AMP BEFORE DROOP
S      DCA \JAL       /STORE PEAK AMPLITUDE
S      NOP            /NOW FIND THE POSITIONS
S      6341           /READ X PEAK LOCATION
S T1,  JMS CVRT       /MASK OFF TWO MSB, COMPLEMENT
S      DCA \JXL       /STORE THE X PEAK LOCATION
S      6342           /READ Y PEAK LOCATION
S T2,  JMS CVRT       /MASK, COMPLEMENT
S      DCA \JYL       /STORE THE Y PEAK LOCATION
          IF (S12-JYL) 315,315,320
315  JYL=JYL-512
          JAL=-JAL
320  CONTINUE
          IF (JXL-390)325,310,310
325  IF (JYL-254)330,310,310
330  CONTINUE
S      JMP I PEAK     /GO BACK TO CALLING PROGRAM

```

```

C      THIS IS THE CONVERT SUBROUTINE FOR READING THE PEAK
C      LOCATIONS.  THE TOP TWO BITS MUST BE MASKED OFF, AND
C      THE REMAINING WORD MUST BE COMPLEMENTED.  THE PEAK
C      LOCATION IS IN THE ACCUMULATOR.

```

```

S CVRT, 0000          /REMEMBER CALLING ADDRESS
S      CHA            /COMPLEMENT
S      AND (1777      /STRIP IT
S      JMP I CVRT     /RETURN

```

```

C THIS IS A ROUTINE TO READ THE VALUE FROM THE A/D CONVERTER
C THE IMPORTANT CODE COMMANDS ARE:
C      6350--CLEAR THE A/D REGISTER
C      6351--LOAD THE A/D MUX
C      6352--START THE A/D CONVERSION
C      6353--READ THE A/D REGISTER
C      6354--SKIP ON CONVERSION COMPLETION
C      6356--LOAD ENABLE REGISTER
C THE MUX CHANNEL USED TO SAMPLE THE PEAK IS 0000.
C GET ON WITH THE PROGRAM!

```

```

S ADC, 0000          /SAVE CALLING ADDRESS
S      6350           /CLEAR THE A/D REGISTER

```



```

S      TAD (32          /SET FOR NO INC,NO INT,UNIPOL,NO TEST
S      6356            /LOAD ENABLE REGISTER WITH 0000
S      6351            /LOAD MUX WITH 0000 FOR CHANNEL 0
S      6352            /START CONVERSION
S DONE, 6354            /SKIP IF A/D DONE
S      JMP DONE         /DOODLE!
S      6353            /READ A/D VALUE INTO AC
S      JMP I ADC        /RETURN

```

```

C THIS IS A PROGRAM TO PROVIDE CROSSHAIRS AND APERTURE COMMANDS
C FOR THE ACME INTERFACE. THE FOUR ARGUMENTS ARE:

```

```

C      IX1 --LEFT HAIR
C      IX2 --RIGHT HAIR
C      IY1 --TOP HAIR
C      IY2 --BOTTOM HAIR

```

```

C THE IMPORTANT CODE COMMANDS FOR THE INTERFACE ARE:

```

```

C      6311 --OUTPUT LEFT CROSSHAIR
C      6312 --OUTPUT RIGHT CROSSHAIR
C      6321 --OUTPUT TOP CROSSHAIR
C      6322 --OUTPUT BOTTOM CROSSHAIR
C      6314 --RESET FRAME FLAG FOR SURE SYNC
C      6324 --SKIP WHEN FLAG SET

```

```

C ALL ADDRESSES ARE LOADED FROM THE ACCUMULATOR.

```

```

C THE RANGE OF VALUES FOR THESE VALUES ARE:

```

```

C      1 < LEFT < RIGHT < 390
C      1 < TOP < BOTTOM < 254

```

```

S AP, 0000            /REMEMBER CALLING ADDRESS

```

```

C CHECK ON HAIR BOUNDS.

```

```

410 IF (IX2-IX1) 500,420,420
420 IF (IY2-IY1) 510,430,430
430 IF (IX1-1) 520,440,440
440 IF (390-IX2) 530,450,450
450 IF (IY1-1) 540,460,460
460 IF (254-IY2) 550,470,470

```

```

470 CONTINUE

```

```

S      CLA

```

```

S      TAD \IX1          /LOAD LEFT HAIR

```

```

S      6311             /SHOVE IT OUT

```

```

S      TAD \IX2          /LOAD RIGHT HAIR

```

```

S      6312             /SHOVE IT

```

```

S      TAD \IY1          /LOAD TOP HAIR

```

```

S      6321             /SHOVE IT

```

```

S      TAD \IY2          /LOAD BOTTOM HAIR

```

```

S      6322             /SHOVE IT

```

```

S      JMP I AP          /RETURN TO CALLING PROGRAM

```

```

500 WRITE (1,505)

```

```

505 FORMAT(15HL/R WRONG ORDER)

```

```

GO TO 560

```

```

510 WRITE (1,515)

```

```

515 FORMAT(15HT/B WRONG ORDER)

```

```

GO TO 560

```

```

520 WRITE (1,525)

```

```

525 FORMAT(13HL/R TOO SMALL)

```

```

GO TO 560

```

```

530 WRITE (1,535)

```

```

535 FORMAT(13HL/R TOO LARGE)

```

```

GO TO 560

```

```

540 WRITE (1,545)

```

```

545 FORMAT(13HT/B TOO SMALL)

```

```

GO TO 560

```

```

550 WRITE (1,555)

```

```

555 FORMAT(13HT/B TOO LARGE)

```

```

560 WRITE (1,570)IX1,IX2,IY1,IY2

```

```

570 FORMAT(12HAP ERROR: L=,I7,4X,2HR=,I7,4X,2HT=,I7,4X,2HB=,I7)

```

```

S      JMP I AP          /RETURN

```

```

600 CONTINUE

```

```

END

```

# **MISSION** **of** **Rome Air Development Center**

RADC plans and conducts research, exploratory and advanced development programs in command, control, and communications (C<sup>3</sup>) activities, and in the C<sup>3</sup> areas of information sciences and intelligence. The principal technical mission areas are communications, electromagnetic guidance and control, surveillance of ground and aerospace objects, intelligence data collection and handling, information system technology, ionospheric propagation, solid state sciences, microwave physics and electronic reliability, maintainability and compatibility.